Original Article

Bioinformatics analysis of immune infiltrates and tripartite motif (*TRIM*) family genes in hepatocellular carcinoma

Jun Cao[1#], Bingbing Su[1#], Rui Peng[1#], Hao Tang[1], Daoyuan Tu[1], Yuhong Tang[1], Jie Zhou[1], Guoqing Jiang[1], Shengjie Jin[1], Qian Wang[1], Aoqing Wang[1], Renjie Liu[1], Qiangwei Deng[2], Chi Zhang[1,3], Dousheng Bai[1,3]

[1]Department of Hepatobiliary Surgery, Clinical Medical College, Yangzhou University, Yangzhou, China; [2]Chenzhou municipal Hospital of Chinese Medicine, Chenzhou, China; [3]General Surgery Institute of Yangzhou, Yangzhou University, Yangzhou, China

Contributions: (I) Conception and design: D Bai, C Zhang, J Cao, B Su, R Peng; (II) Administrative support: D Bai, C Zhang; (III) Provision of study materials or patients: J Cao, B Su, R Peng, H Tang, D Tu, Y Tang, J Zhou; (IV) Collection and assembly of data: S Jin, R Liu, G Jiang, Q Wang, A Wang, Q Deng; (V) Data analysis and interpretation: J Cao, B Su; (VI) Manuscript writing: All authors; (VII) Final approval of manuscript: All authors.

[#]These authors contributed equally to this work and should be considered as co-first authors.

Correspondence to: Dousheng Bai; Chi Zhang. Department of Hepatobiliary Surgery, Clinical Medical College, Yangzhou University, 98 West Nantong Rd, Yangzhou 225000, China. Email: drbaidousheng@yzu.edu.cn; 18051062769@yzu.edu.cn.

Background: The tripartite motif (*TRIM*) family are important members of the Gene-finger-containing E3 ubiquitin-conjugating enzyme and are involved in the progression of hepatocellular carcinoma (HCC). Previous studies have largely focused on gene expression and molecular pathways, while the underlying role of the *TRIM* family in the tumor immune microenvironment (TIME) remains poorly understood.

Methods: We systematically explored the correlations of prominent *TRIM* genes with immune checkpoints and immune infiltrates in 231 HCC samples [International Cancer Genome Consortium (ICGC) cohort (n=231); The Cancer Genome Atlas (TCGA) cohort (n=370)]. A prognostic risk model was constructed using the least absolute shrinkage and selection operator (LASSO) algorithm and multivariate Cox regression analysis in the ICGC cohort. Kaplan-Meier curves based on the overall survival (OS) were used to assess differences in survival between clusters. We utilized gene set variation analysis (GSVA) to characterize the differences in biological functions. Based on univariate and multivariate Cox progression analysis, we developed a risk score signature and verified its reliability and validity. The Tumor Immune Single-cell Hub (TISCH) single-cell database was employed to evaluate the correlation of *TRIM* genes with the tumor microenvironment.

Results: Cluster 1 was preferentially associated with a favorable prognosis (P<0.001). The amino acid, fatty acid, and drug metabolism pathways were significantly enriched in cluster 2. A prognosis risk score project was established and evaluated based on the 9 independent prognostic genes (all P<0.05). The immune score and stromal scores of patients with low-risk scores were greater than those of patients with high-risk scores (all P<0.001). However, patients with a high-risk score exhibited lower responses to immune checkpoint inhibitors (ICIs), sorafenib, and transarterial chemoembolization (TACE) treatment (all P<0.05). Consistently, *TRIM* genes showed the same influence in the external TCGA cohort. *TRIM* gene-based signatures were implicated in TIME and their copy-number alterations dynamically impacted the abundance of tumor-infiltrating immune cells.

Conclusions: Our findings revealed that MID1, TRIM5, TRIM22, TRIM28, TRIM 31, TRIM37, TRIM38, TRIM47, and TRIM74 could serve as efficient prognostic biomarkers and therapeutic targets in HCC. The identified *TRIM* gene-based signatures could serve as important TIME mediators in HCC, potentially increasing immune treatment efficacy.

Keywords: Hepatocellular carcinoma (HCC); tripartite motif (*TRIM*) genes; tumor immune microenvironment (TIME); immune infiltrates; immunotherapy

Submitted Jul 05, 2022. Accepted for publication Aug 05, 2022.
doi: 10.21037/jgo-22-619
View this article at: https://dx.doi.org/10.21037/jgo-22-619

Introduction

Hepatocellular carcinoma (HCC) is the most common primary liver malignancy and the world's fourth leading cause of cancer-related mortality (1). Liver transplantation and hepatectomy are curative treatments for HCC, and the indications have been safely expanded (2,3). However, some tumors are still too advanced to be cured by surgical resection and orthotopic liver transplantation at diagnosis. Therefore, it is important to administer palliative treatments to achieve downstaging for surgical therapy or delay the progression of tumors. Combination therapy improves the prognosis outcomes of patients with advanced HCC better than single-agent therapy (4), implying that combined therapy could be a promising treatment option for some HCC patients.

In the past few decades, cancer immunotherapy has become one of the most effective treatments and has been validated in various tumors (5,6). Since the advent of immune checkpoint inhibitors (ICIs), the concept of normalizing the tumor immune microenvironment (TIME) by correcting dysfunctions of the immune response has drawn attention again to immunotherapy. Immune checkpoint therapy, which is at the forefront of immunotherapy, has demonstrated clinical activity in several malignancies, including HCC, although the response rate to ICIs varies in patients (7,8). The encouraging results from clinical trials of immune checkpoint therapy have resulted in increased clinical implementation in various types of cancer, including HCC. However, only approximately 20% of advanced HCC patients benefit from ICIs, and most of them have disease progression after 3–9 months (9). These results indicate that a substantial proportion of patients treated with ICIs suffer primary or acquired resistance. Therefore, studying the underlying mechanism and maximizing the curative effect of immune checkpoint therapy has become a focus in the field of HCC treatment.

Members of the tripartite motif (TRIM) protein family are engaged in a wide range of cellular functions and share several functional characteristics (10). The *TRIM* family, consisting of roughly 80 members, is structurally a highly conserved gene family whose family members all contain the RING finger domain, a basic composition of 1 or 2 zinc-finger domains called B boxes, and a coiled-coil region (11). Diverse C-terminal domains determine the primary structural distinctions within the *TRIM* family, and *TRIM* proteins are divided into 11 classes based on their C-terminus (from C-I to C-XI) (12). To date, *TRIM* proteins have been shown to regulate cell proliferation (13,14), facilitate or prevent cancer cell transformation (15), and directly interact with innate immunity (11), among many other roles. It has been shown that multiple *TRIM* genes play a significant function in liver cancer development as well as its immunotherapy (16,17). However, the relationship between *TRIM* genes and the effect of treatment as well as prognosis in HCC is not clear.

Although single TRIM family gene has been investigated in various solid tumors, no systematical and comprehensive analysis has been performed to identify the role of TRIMs in HCC. Our study aimed to systematically assess *TRIM* family correlations with prognosis, checkpoints, and TIME in HCC. The relationships between clustering subgroups, risk models, checkpoints, immune scores, and immune cell infiltration, and the responsiveness of sorafenib and transarterial chemoembolization (TACE) treatment were subsequently thoroughly analyzed based on *TRIM* family gene-related signatures to further investigate *TRIM* genes' effect on TIME. The development of risk models for *TRIM* genes is vital for helping to improve risk stratification and clinical decision-making in HCC. We present the following article in accordance with the TRIPOD reporting checklist (available at https://jgo.amegroups.com/article/view/10.21037/jgo-22-619/rc).

Methods

Datasets

The International Cancer Genome Consortium (ICGC) and The Cancer Genome Atlas (TCGA) databases (https://daco.icgc.org/ and https://portal.gdc.cancer.gov/) were used to obtain RNA sequencing (RNA-seq) transcriptome data and clinical data of HCC patients. The inclusion criteria were: (I) histologically confirmed HCC, and (II) data on mRNA expression profiles and overall survival (OS) available at the same time. Ultimately, 231 samples

Table 1 Clinicopathological features of patients in TCGA and ICGC cohorts

Variables	Datasets, n (%)	
	TCGA	ICGC
Age		
<53 years	101 (27.3)	20 (8.7)
≥53 years	269 (72.7)	211 (91.3)
Gender		
Female	121 (32.7)	61 (26.4)
Male	249 (67.3)	170 (73.6)
Grade		
G1	55 (14.9)	–
G2	177 (47.8)	–
G3	121 (32.7)	–
G4	12 (3.2)	–
Stage		
Stage 1	171 (46.2)	36 (15.6)
Stage 2	85 (23.0)	105 (45.5)
Stage 3	85 (23.0)	71 (30.7)
Stage 4	5 (1.4)	19 (8.2)
M		
M0	266 (71.9)	–
M1	4 (1.1)	–
T		
1	181 (48.9)	–
2	93 (25.1)	–
3	80 (21.6)	–
4	13 (3.5)	–

TCGA, The Cancer Genome Atlas; ICGC, International Cancer Genome Consortium.

of HCC were acquired, together with clinicopathological characteristics such as age, sex, grade, and TNM stage. A total of 231 ICGC HCC patients were assigned to the training cohort, while 370 TCGA patients were assigned to the validation cohort. The baseline clinicopathological features are shown in *Table 1*. The GSE109211 and GSE104580 datasets from the Gene Expression Omnibus (GEO; https://www.ncbi.nlm.nih.gov/geo/) database were used to analyze the responsiveness of sorafenib, TACE, and ICI treatment. The study was conducted in accordance with the Declaration of Helsinki (as revised in 2013).

TRIM genes selection

Based on previously published literature, 62 *TRIM* genes were selected (11). On the basis of mRNA expression results of liver hepatocellular carcinoma (LIHC) from ICGC, a total of 62 *TRIM* genes were identified. Next, the differential expression of 62 *TRIM* genes in tumor tissues and adjacent normal tissues was analyzed.

Bioinformatics analysis

We used the "ConsensusClusterPlus" program to classify HCC patients into different subtypes in order to explore the biological functions of *TRIM* genes in HCC. To examine gene expression patterns among different HCC subtypes, principal component analysis (PCA) was performed using R (v4.1.0). Pathways analysis for different HCC subtypes was carried out using the R software package "GSVA".

The immune score for each patient was estimated using the R "estimate package" and an algorithm (18). Cell-type identification by calculating relative subsets of RNA transcripts (CIBERSORT; https://cibersort.stanford.edu/) was used to develop the fraction of 22 immune cell types for each tumor specimen. With 1,000 permutations, the samples were chosen based on $P<0.05$.

In the ICGC training cohort, we performed K-M survival analysis for all *TRIM* genes, and we used least absolute shrinkage and selection operator (LASSO) regression analysis to identify predictive risk signatures for above *TRIM* genes ($P<0.05$). Ten cross-validations were used to select suitable values for the penalty parameter. The LASSO regression approach yielded the coefficients, and the risk score was obtained using the following formula: Riskscore=∑i=1ncodfi*xi where codfi is the coefficient and xi is the transformed relative expression value of each selected *TRIM* genes. This formula was used to generate a risk score for each patient in the training and validation cohorts. The samples were then separated into high-risk and low-risk categories based on the cutoff (median value).

Data from GEO and Array Express were collected by Tumor Immune Single-cell Hub (TISCH) to formulate a single-cell RNA-seq (scRNA-seq) atlas. TISCH compares different patients, therapy and response groups, tissue origins, cell types, and even cancer types by visualizing gene expression across several data sets at the single-cell or

cluster level. In this study, we employed TISCH datasets to unravel the TME heterogeneity of 8 *TRIM* genes at the single-cell level.

The role of copy number alternations (CNAs) of the *TRIM* family on immune cell infiltration levels was evaluated by applying the Tumor Immune Estimation Resource (TIMER, https://cistrome.shinyapps.io/timer/).

Statistical analysis

R version 4.1.0 and GraphPad Prism 9.2 were used for statistical analysis. A Student's *t*-test, chi-square test, and Mann-Whitney-Wilcoxon test were used for comparisons between 2 groups, and a one-way analysis of variance (ANOVA) test was utilized for analysis with multiple comparisons. Survival curves were generated and compared using the Kaplan-Meier method. Univariate and multivariate analyses were conducted with Cox proportional hazards regression models. Receiver operating characteristic (ROC) curves were employed to compare the predictive accuracy of the *TRIM* gene-relevant signatures. P<0.05 (two-sided) indicated statistical significance.

Results

Expression of TRIM genes in HCC

Based on the ICGC dataset, we systematically investigated the expression patterns of 62 *TRIM* genes between HCC (n=240) and normal tissues (n=197) to assess the biological function of *TRIM* genes in the initiation and development of HCC. The expression levels of *TRIM* genes in HCC and normal tissues were evident (Figure S1A,S1B). The expression levels of most *TRIM* genes (45 of 62) were higher in HCC tissues than in normal adjacent tissues. Some *TRIM* genes (7 of 62) were lower in HCC tissues than in normal tissues (Figure S1A,S1B, Table S1). Additionally, there were also *TRIM* genes (10 of 62) with no statistically significant difference (P>0.05). The above results revealed that *TRIM* genes might possess essential biological roles in HCC development.

Significant correlation of consensus clustering for TRIM genes with the characteristics and survival of HCC patients

To achieve optimum clustering stability, k=2 was determined, and the samples from 231 patients with HCC were divided into 2 subgroups (*Figure 1A*). Individual *TRIM* gene expression was lower in cluster 1 than it was in cluster 2 (*Figure 1B*). Next, the clinicopathological characteristics of the 2 subgroups were compared (*Figure 1B*). Cluster 2 was more significantly related to higher stage (P<0.01) and higher mortality than cluster 1. Cluster 1 had a superior OS (P<0.001; *Figure 1C*). The results of PCA found that the gene expression profiles of the 2 groups were well differentiated (*Figure 1D*).

Association of immune check points with TRIM family

We looked at differential expression in 2 subtypes and the relationship between immune checkpoints and *TRIM* genes to see whether immune checkpoints were related. The expression level of *KIR2DL1*, *KIR2DL3*, *KIR2DL2*, *KLRC1*, *LAG3*, *CD274*, *CTLA4*, and *TIGIT* were downregulated in HCC tissues compared with normal tissues (P<0.05; *Figure 2A*). *CTLA4*, *HAVCR2*, and *PDCD1* expression levels in cluster 2 were significantly higher than in cluster 1 (P<0.05; *Figure 2B*). NT5E expression, on the other hand, was lower in cluster 2 than in cluster 1 (P<0.05; *Figure 2B*). We then analyzed the correlation between *TRIM* genes and the immune checkpoints (*PDCD1*, *NT5E*, *HAVCR2*, and *CTLA4*) in ICGC and TCGA datasets, which showed that a number of *TRIM* genes had a significant correlation with immune checkpoints, as shown in *Figure 2C*,*2D*. The above results suggested that *TRIM* family genes may improve immunotherapy for HCC.

Consensus clustering for TRIM genes associated with distinct immune cell infiltration

To investigate the effect of *TRIM* genes on the TIME of HCC, we compared the immune infiltrate levels in cluster 1 and cluster 2 (*Figure 2E*). This analysis showed a significant difference in naive B cells, memory B cells, regulatory T cells (Tregs), gamma delta T cells, M0 macrophages, M1 macrophages, resting dendritic cells, and stromal score between the 2 clusters (*Figure 2E*). Cluster 1, with a higher stromal score, had a better prognosis than cluster 2, with a lower stromal score (P<0.05). We further performed gene set variation analysis (GSVA) and the results showed that the spliceosome, homologous recombination, and DNA replication pathway might be implicated in the distinct TIME of cluster 2 (P<0.0001; *Figure 3A*), while amino acid metabolism, fatty acid metabolism, and the drug metabolism cytochrome P450 pathway might be implicated in the distinct TIME of cluster 1 (P<0.0001; *Figure 3A*, Table S2).

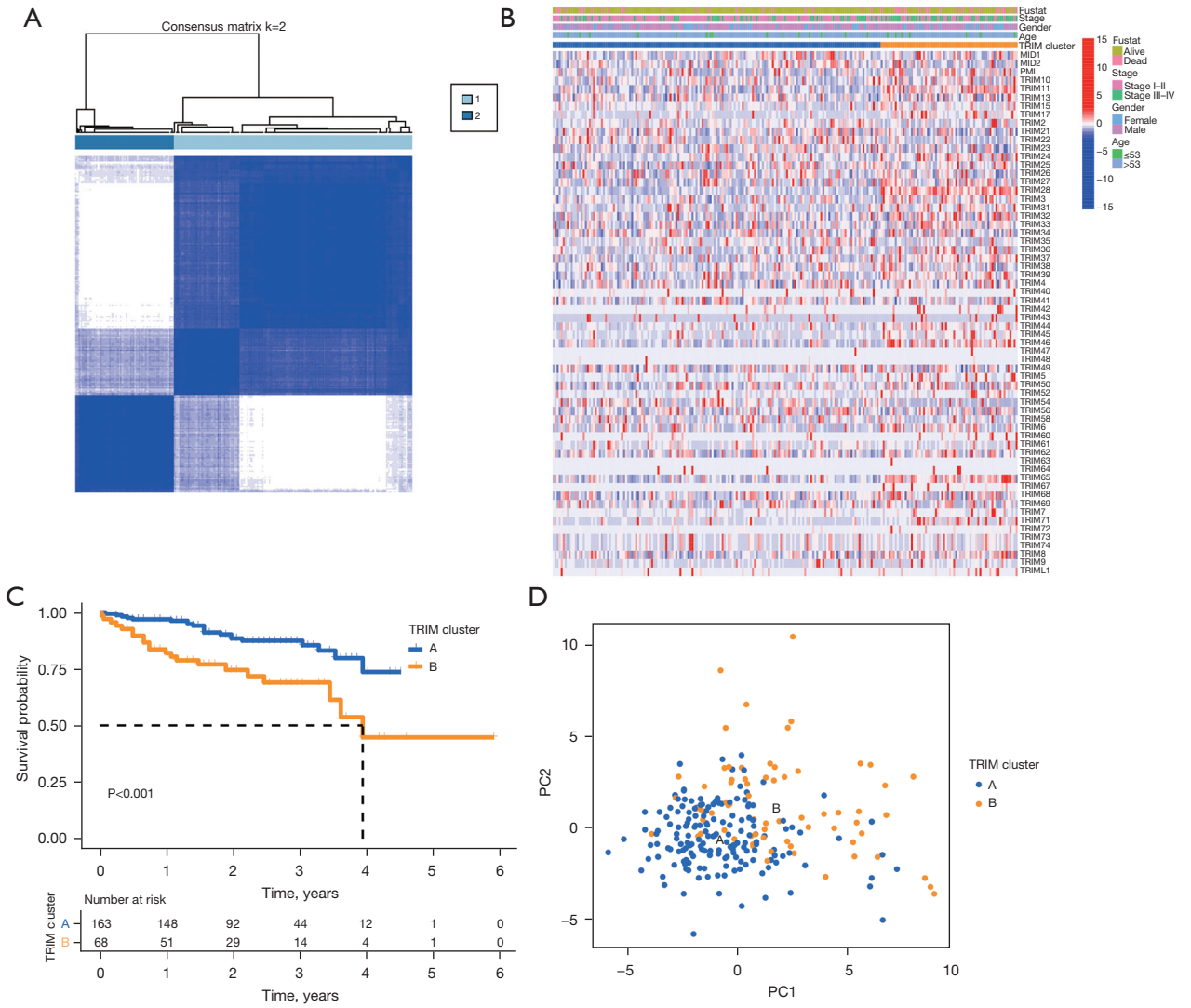

Figure 1 Differential clinicopathological features and survival of HCC in cluster 1/2 subtypes in ICGC cohort. (A) Consensus clustering matrix for k=2. (B) Heatmap and clinicopathologic features of the 2 clusters (cluster 1/2). (C) Kaplan-Meier curves of OS for patients with HCC in 2 clusters (cluster 1/2). (D) Principal component analysis of the total mRNA expression profile in 231 patients with HCC. HCC, hepatocellular carcinoma; ICGC, International Cancer Genome Consortium; OS, overall survival; TRIM, tripartite-motif; PC, principal component.

Hence, the metabolism-related signaling pathways might be implicated in the distinct TIME of cluster 1.

Construction and validation of prognostic signatures for TRIM genes

A total of 231 ICGC HCC patients were assigned to the training group, while 370 TCGA patients were assigned to the validation cohort (*Table 1*). We conducted univariate analysis for *TRIM* genes, and the results showed that 12 *TRIM* genes (*MID1*, *TRIM11*, *TRIM21*, *TRIM22*, *TRIM24*, *TRIM28*, *TRIM31*, *TRIM37*, *TRIM42*, *TRIM47*, *TRIM5*, are *TRIM74*) were related to survival in HCC (all P<0.05; *Figure 3B*, Table S3).

To accurately predict the clinical prognosis of HCC patients, we performed K-M survival analysis for all *TRIM* genes, and we used least absolute shrinkage and selection operator (LASSO) regression analysis to identify predictive risk signatures for above *TRIM* genes (P<0.05). The results showed that 9 *TRIM* genes, namely *MID1*, *TRIM38*,

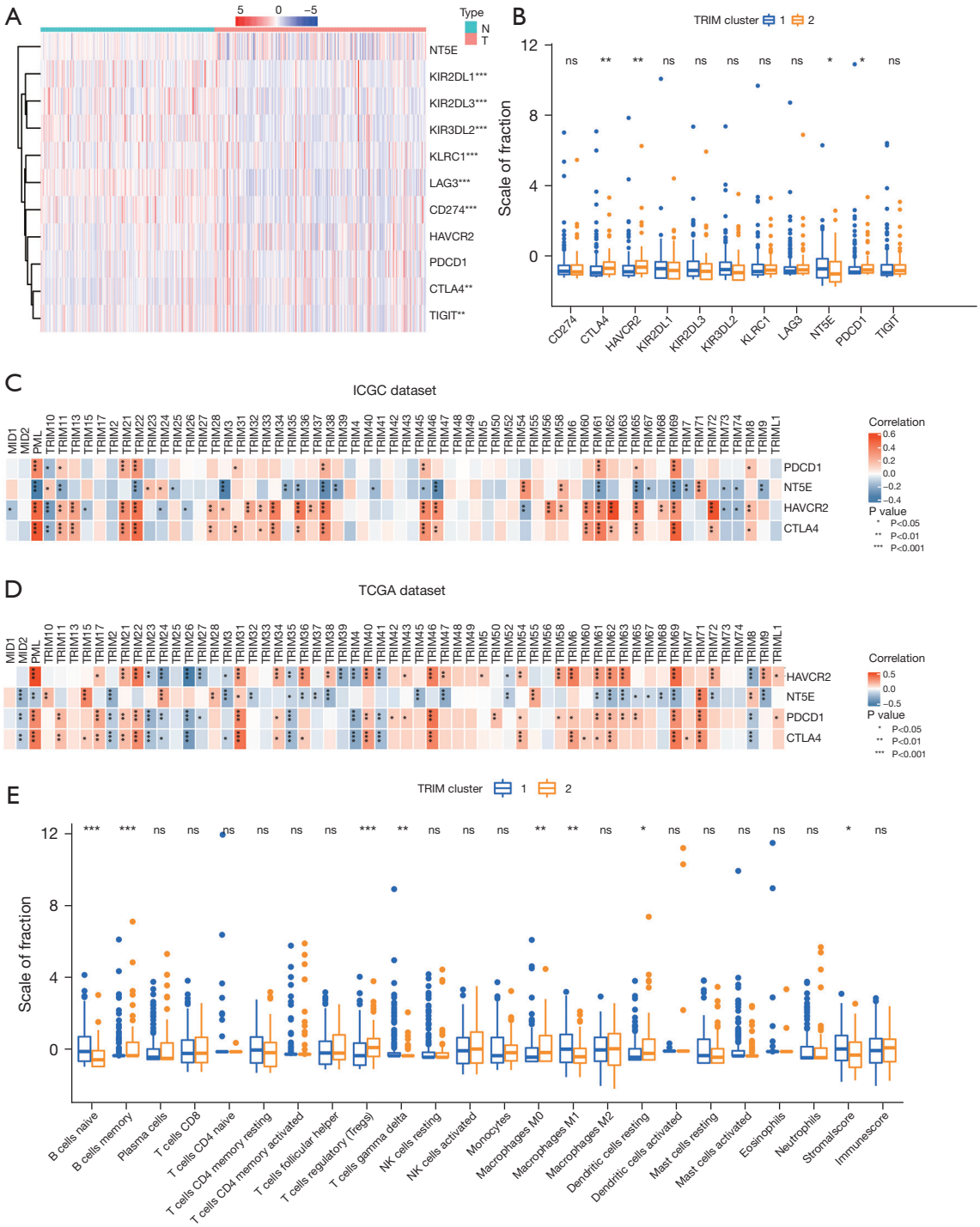

Figure 2 Association of immune check points with *TRIM* genes and the landscape of immune cell infiltration in HCC. (A) Tumor *vs.* normal; (B) cluster 1 *vs.* cluster 2; (C) ICGC dataset; (D) TCGA dataset; (E) landscape of immune cell infiltration in cluster 1/2. *P<0.05, **P<0.01, and ***P<0.001. TRIM, tripartite-motif; HCC, hepatocellular carcinoma; ICGC, International Cancer Genome Consortium; TCGA, The Cancer Genome Atlas; ns, no significance.

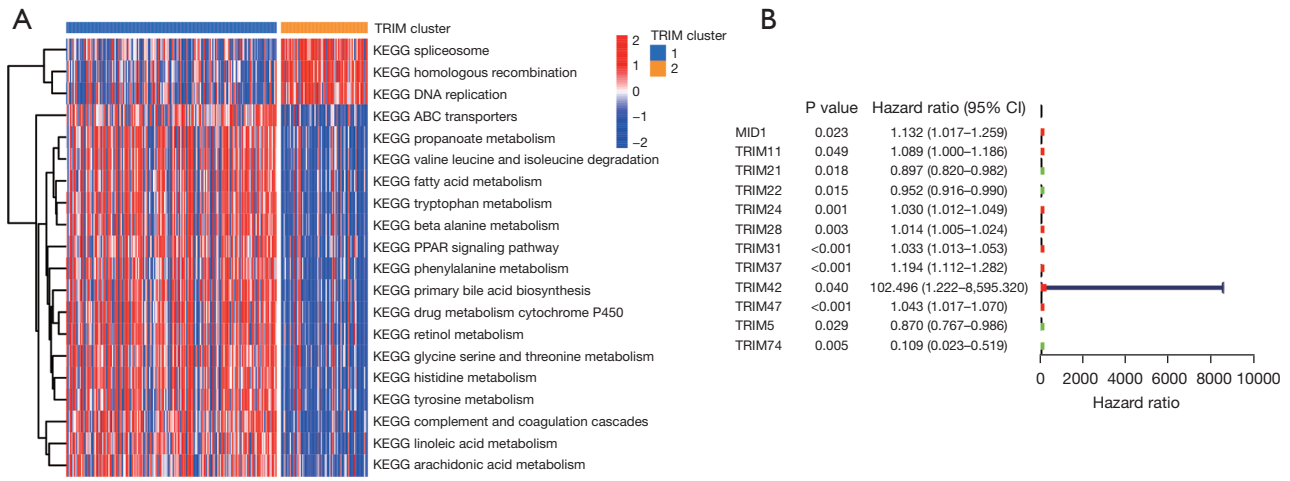

Figure 3 The potential regulatory mechanisms resulting in differences in TIME. (A) The potential regulatory mechanisms resulting in differences in TIME between the 2 subgroups by performing GSVA; (B) univariate analyses in the ICGC training cohort. TIME, tumor immune microenvironment; GSVA, gene set variation analysis; ICGC, International Cancer Genome Consortium.

TRIM37, *TRIM47*, *TRIM24*, *TRIM28*, *TRIM22*, *TRIM5*, and *TRIM74*, were identified. The median risk score (median =0.5656) was then used to separate patients into low- and high-risk groups (Table S4). The distribution of risk scores, OS, OS status, and expression profiles of the 9 *TRIM* gene-based signatures in the ICGC training and TCGA validation cohorts are shown in *Figure 4*. The heatmap data showed that *TRIM* genes, including *MID1*, *TRIM28*, *TRIM31*, *TRIM37*, and *TRIM47*, were substantially expressed in the high-risk group (*Figure 4*). In the ICGC training and TCGA validation cohorts, the low-risk group had a longer OS than the high-risk group (P<0.05; *Figure 4*). We then performed univariate and multivariate analyses and found that risk score was an independent prognostic factor in the ICGC and TCGA datasets (all P<0.05; *Figure 5*). We compared the respective area under curve (AUC) values in 1-, 3-, and 5-year ROC curve analyses to determine the prognostic accuracy of our model. The 1-, 3-, and 5-year AUC values for the 9 risk signatures in the ICGC training cohort were 0.789, 0.827, and 0.694, respectively (*Figure 5*), and 0.642, 0.571, and 0.533 in the TCGA dataset, respectively (*Figure 5*). Our model, based on the 9 *TRIM* genes, demonstrated favorable discrimination performance for the prognosis of patients with HCC, as evidenced by the AUC values. The results of PCA analysis corroborated the preceding findings (Figure S2). These findings suggested that the risk score derived from the 9 risk signatures might reliably predict HCC patients' prognosis.

Risk scores correlated with stage, immune score, TRIM cluster, and therapies in HCC

The association between risk score and clustering subtypes, stage, immune score, estimate score, stromal score, tumor purity, and OS status was also investigated. The cluster 2 risk score was significantly greater than the cluster 1 risk score (P<0.001; *Figure 6*). The high-risk group had a significantly lower immune score and higher TNM stage than the low-risk group (P<0.01; *Figure 6*).

The heatmap depicted the expression levels of 9 *TRIM* genes in the ICGC training cohort's high- and low-risk groups (*Figure 6*). The high-risk group had lower levels of *TRIM38*, *TRIM22*, *TRIM5*, and *TRIM74* expression than the low-risk group. *TRIM31*, *TRIM47*, *TRIM28*, *TRIM37*, and *MID1* expression levels were low in the low-risk group. In addition, we analyzed the correlation of the 9 prognostic *TRIM* genes with TNM stage in the ICGC and TCGA datasets, and the result showed that in the ICGC dataset, there was a clear positive correlation between the expression of *TRIM28* and *TRIM47* and TNM stage, and similar results could be obtained in the TCGA dataset (Figure S3).

Immunotherapy, TACE, and molecularly targeted therapies have been widely used in the treatment of patients with HCC and contribute to the prognosis of patients. We investigated whether *TRIM* genes harbored the same influence on ICIs, sorafenib, and TACE treatment in additional HCC cases. First, we employed the tumor immune dysfunction and exclusion (TIDE)

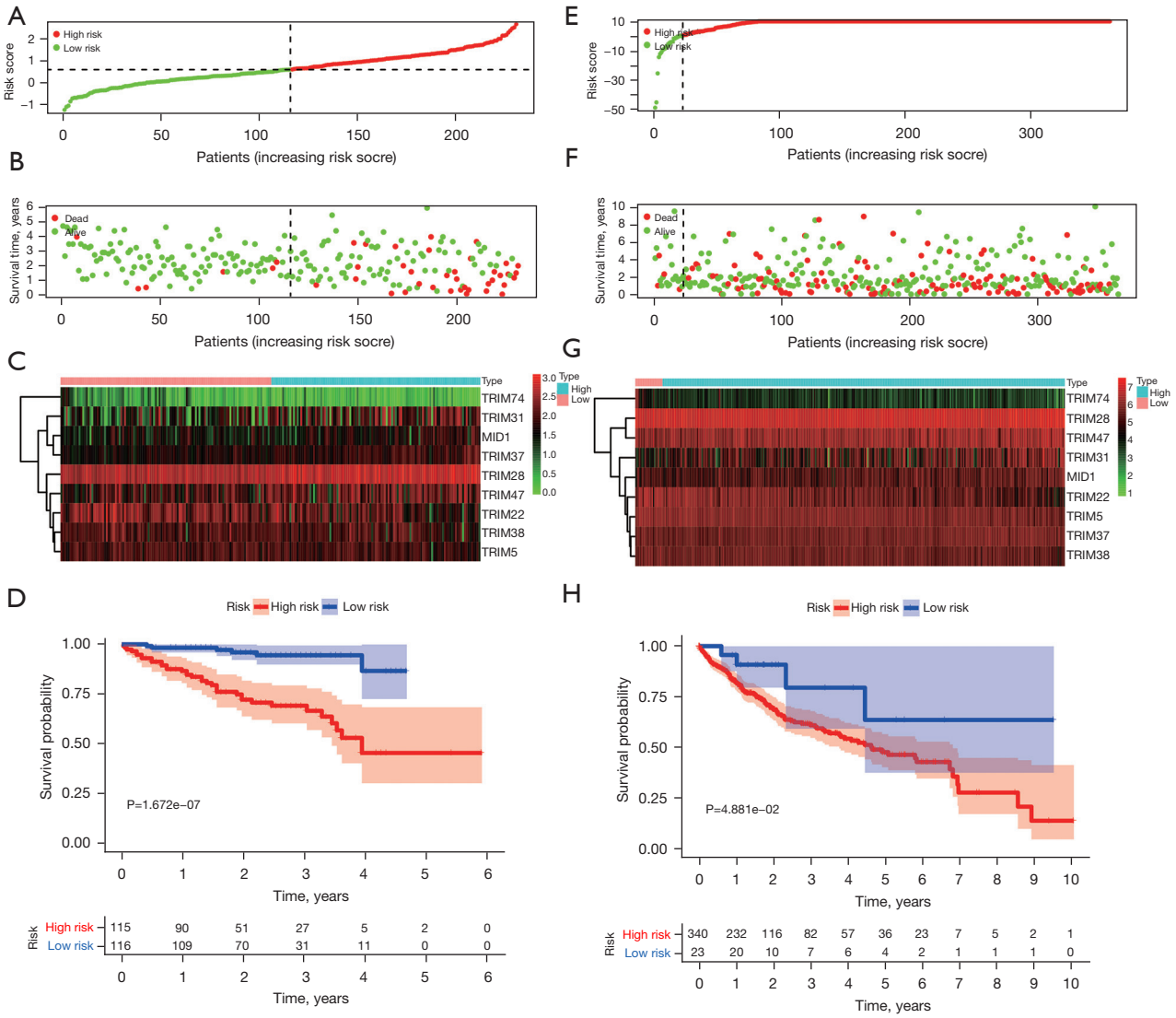

Figure 4 Construction and validation of prognostic signatures of *TRIM* genes in ICGC and TCGA cohorts. (A-D) Distribution of risk score, OS, and OS status and heatmap of the 9 prognostic *TRIM* genes in the ICGC training cohort; (E-H) distribution of risk score, OS, and OS status and heatmap of the 9 prognostic *TRIM* genes in the TCGA validation cohort. TRIM, tripartite-motif; ICGC, International Cancer Genome Consortium; TCGA, The Cancer Genome Atlas; OS, overall survival.

score, a scoring system that integrates 2 tumor immune escape mechanisms, to analyze the response rate of HCC immunotherapy. A high TIDE score indicates a poor treatment effect for ICIs (19). The results showed that the TIDE score of high-risk patients was high, but the response rate of immunotherapy in low-risk patients was higher than that in high-risk patients (87% *vs.* 65%; *Figure 7A*,*7B*). Next, we selected the eligible GEO datasets, GSE109211 and GSE104580, as the external validation cohort. The response to sorafenib was not significantly different from the risk score, but the response rate was significantly higher in low-risk patients than in high-risk patients (42% *vs.* 24%; Figure S4A, *Figure 7C*, Table S5), which was possibly due to the small number of patients who responded to sorafenib. In addition, the response to TACE was significantly different from the risk score, and the response rate was higher in low-risk patients than in high-risk patients (65% *vs.* 39%; Figure S4B, *Figure 7D*, Table S6).

Single-nucleotide variant (SNV) mutations are associated

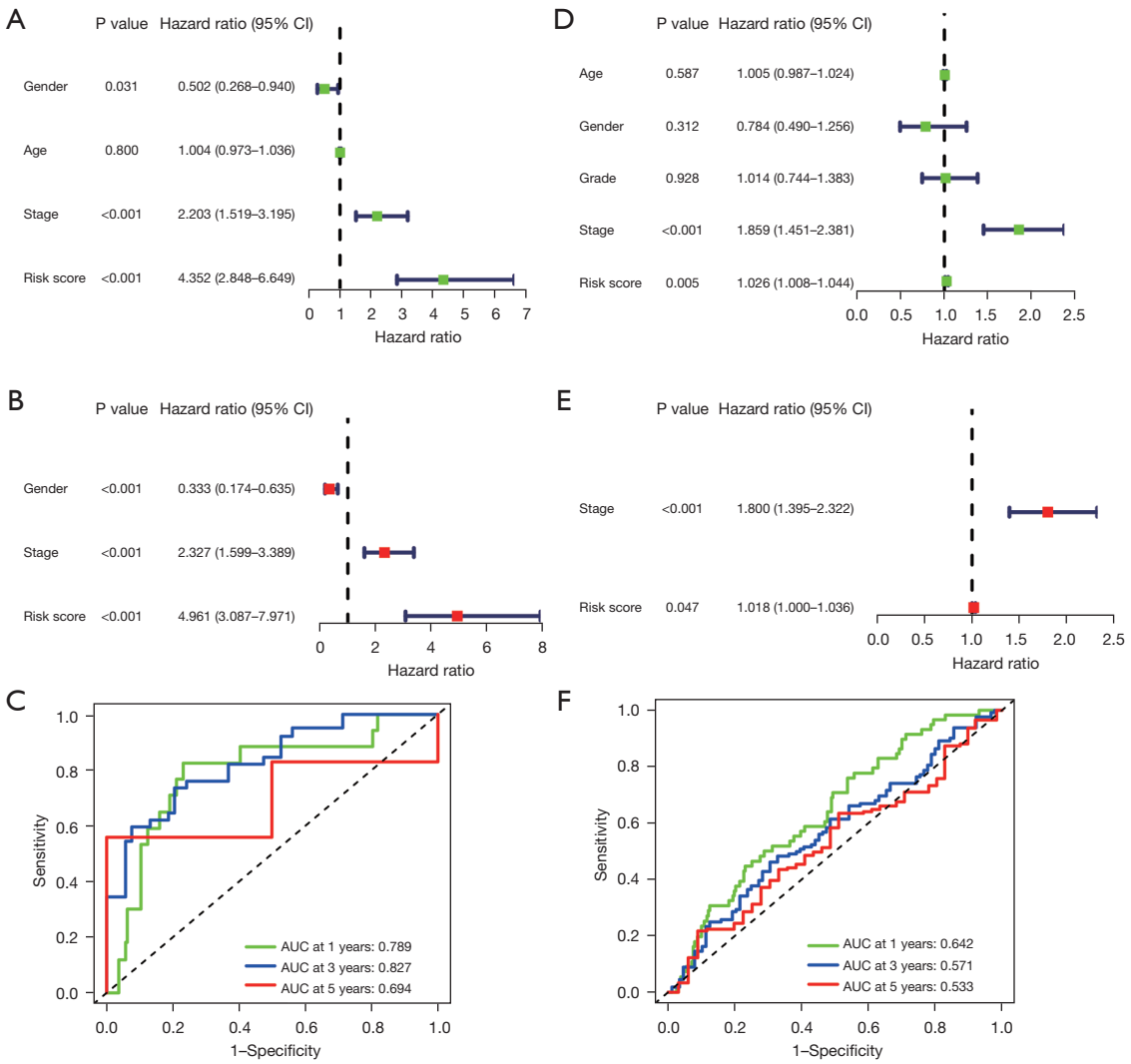

Figure 5 Univariate, multivariate Cox regression and ROC analyses in the 2 cohorts. Univariate (A) and multivariate (B) Cox regression analyses in the ICGC training cohort; univariate (D) and multivariate (E) Cox regression analyses in the TCGA validation cohort; receiver operating characteristic curves of 1, 3, and 5 years based on the risk score in the ICGC training cohort (C) and TCGA validation cohort (F). ICGC, International Cancer Genome Consortium; TCGA, The Cancer Genome Atlas.

with HCC treatment efficacy prediction and immune infiltration (20), so specific mutations in high- and low-risk groups may bring benefits for the prognosis of patients. We compared HCC samples from the low *TRIM* score subgroup to those from the high *TRIM* score subgroup in terms of substantially modified genes (*SMG*). The *SMG* mutational landscapes revealed that in the high *TRIM* score group, TP53 (17% *vs.* 47%) had greater somatic mutation rates, whereas in the low *TRIM* score group, CTNNB1 (34% *vs.* 23%) had higher somatic mutation rates (Figure S5A,S5B).

Correlation between TRIM genes and the TISH database

We used TISCH to investigate the expression of the *TRIM* genes in the HCC tumor microenvironment at the single-cell level (*Figure 8A-8I*). In LIHC_GSE140228, most *TRIM* genes were mainly expressed in immune cells, including B cells, plasma cells, exhausted CD8T (Tex) cells, CD8T cells, CD4 conventional T (Tconv) cells, mono/macrophages, mast cells, Tpolif cells, natural killer (NK) cells, and regulatory T cells. These results suggested that the expression of *TRIM* genes in HCC was closely related

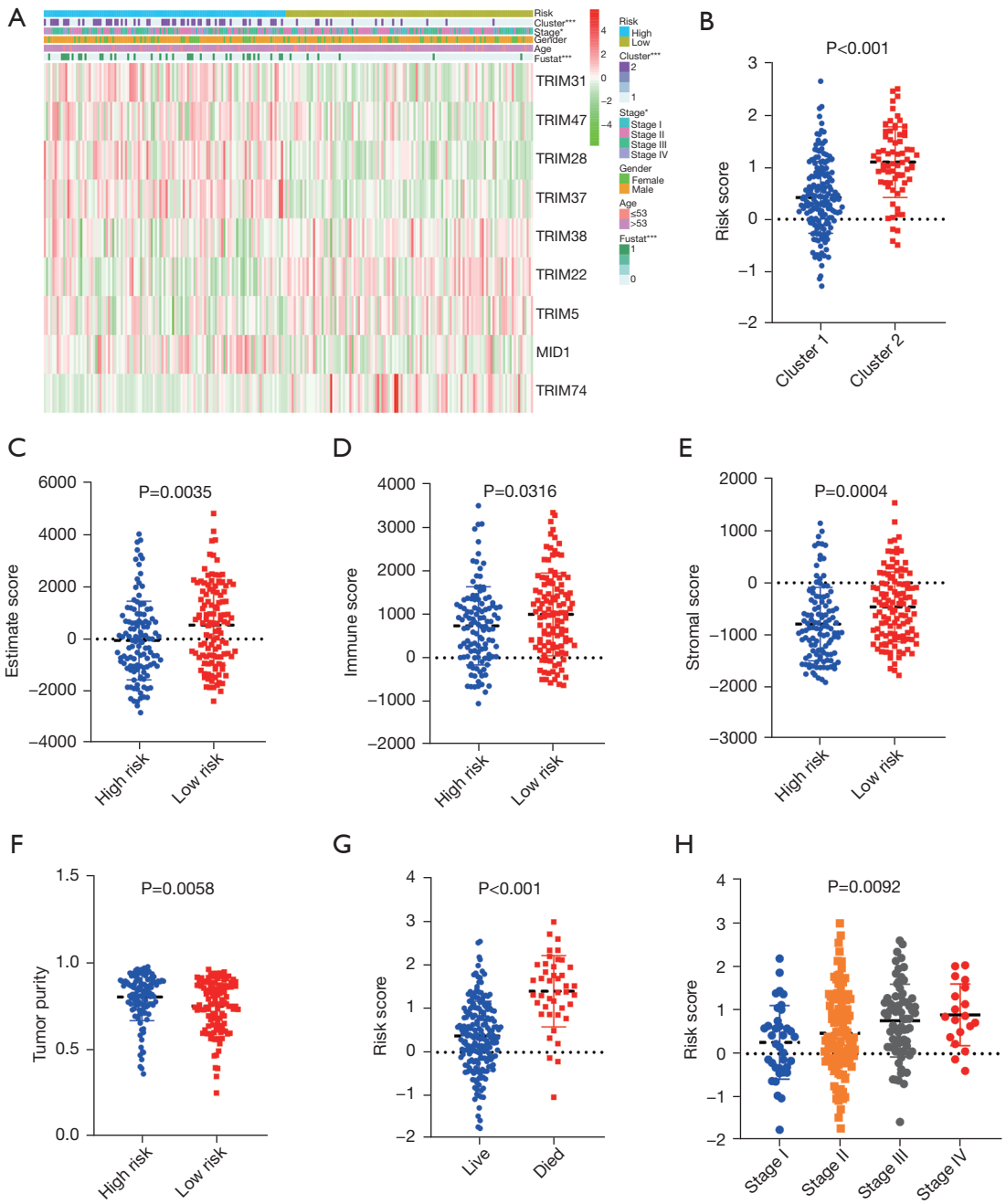

Figure 6 Prognostic risk scores correlated with clinicopathological features, estimate score, stromal score, tumor purity, OS status, TNM stage, and immune score in TCGA training cohort. (A) Heatmap and clinicopathologic features of high- and low-risk groups. (B-H) Distribution of risk scores stratified by cluster 1/2 (B), estimate score (C), immune score (D), stromal score (E), tumor purity (F), OS status (G), and TNM stage (H). *P<0.05, and ***P<0.001. OS, overall survival; TCGA, The Cancer Genome Atlas.

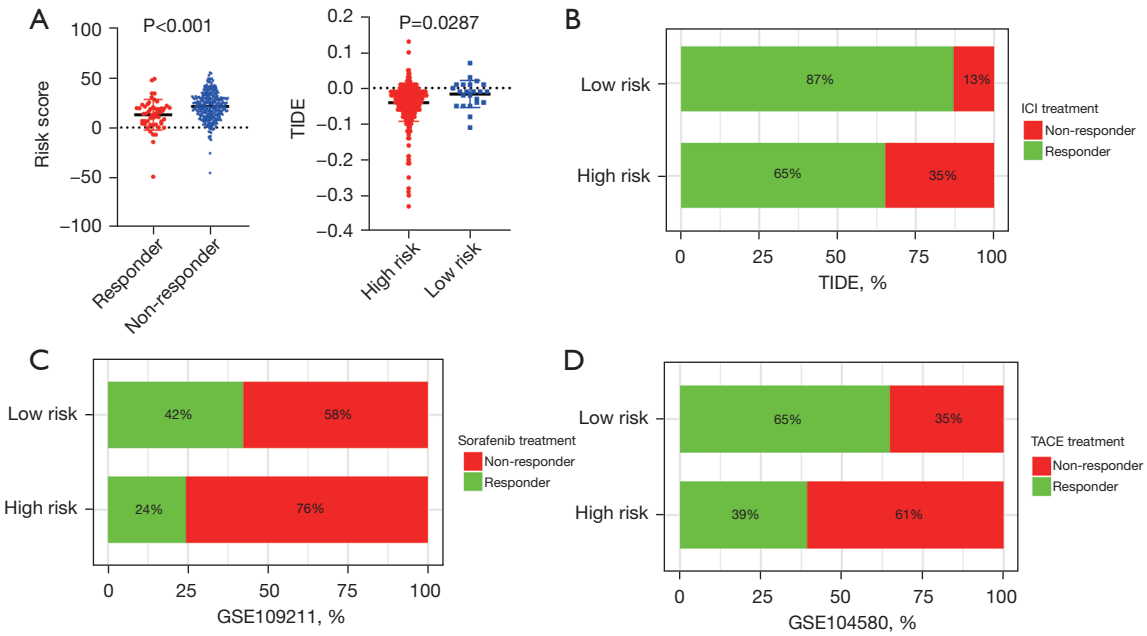

Figure 7 Prognostic risk scores correlated with TIDE score, sorafenib and TACE treatment. (A) Prognostic risk scores correlated with TIDE score; (B) the response to ICI treatment; the response to sorafenib treatment (C) and TACE treatment (D). TIDE, tumor cell dysfunction and exclusion; ICIs, immune checkpoint inhibitors; TACE, transarterial chemotherapy embolization.

to immune cell infiltration (*Figure 8*).

Effect of genetic alterations of the TRIM gene signatures on immune cell infiltration

We used TIMER 2.0 to analyze the relationship of 9 *TRIM* genes with infiltration levels of 6 immune cell types to assess the effect of the 9 *TRIM* genes on the HCC immune microenvironment. The results revealed that a significantly positive correlation was observed between almost all the immune cells and the 9 *TRIM* genes (Figures S6,S7). These results confirmed that *TRIM* gene-based risk signatures were implicated in the TIME of HCC.

Genome instability and immune cell infiltration are both promoted by somatic CNAs. The infiltration levels of B cells, $CD4^+$ T cells, $CD8^+$ T cells, neutrophils, macrophages, and dendritic cells in HCC were significantly impacted by the CNAs of the identified *TRIM* gene signatures, including arm-level deletion and arm-level gain (*Figure 9*). These findings showed that *TRIM* genes were important regulators of TIME in HCC patients.

Finally, we performed copy number variation (CNV) analysis on 9 *TRIM* genes, and the results showed that all 9 genes had acquired mutations greater than deletion mutations (*Figure 10A*). In addition, we labeled the location of the 9 *TRIM* genes on the chromosome, as shown in *Figure 10B*. Further analysis showed that in *MID1*, the alteration frequency of deep deletion and amplification accounted for the vast majority, but in *TRIM5* and *TRIM28*, both accounted for half. In addition, the alteration frequency of amplification occupied almost all of the other *TRIM* genes (*Figure 10C*). The results of the abovementioned studies indicated that the genomic and transcriptomic landscapes had significant differences and connections.

Discussion

The expression patterns, prognostic values, and effects on TIME of the *TRIM* genes in HCC were investigated in this study. In HCC tissues, the expression of 45 *TRIM* genes increased significantly, while the expression of 7 *TRIM* genes dropped dramatically. By using consensus clustering for *TRIM* genes, we were successful in identifying subgroups of HCC: cluster 1 and cluster 2. The cluster subtype affected the prognosis and different clinicopathological features of HCC and was closely related to immune cell infiltration levels. We characterized the effects of differential *TRIM* genes on different HCC subtypes by clustering *TRIM*

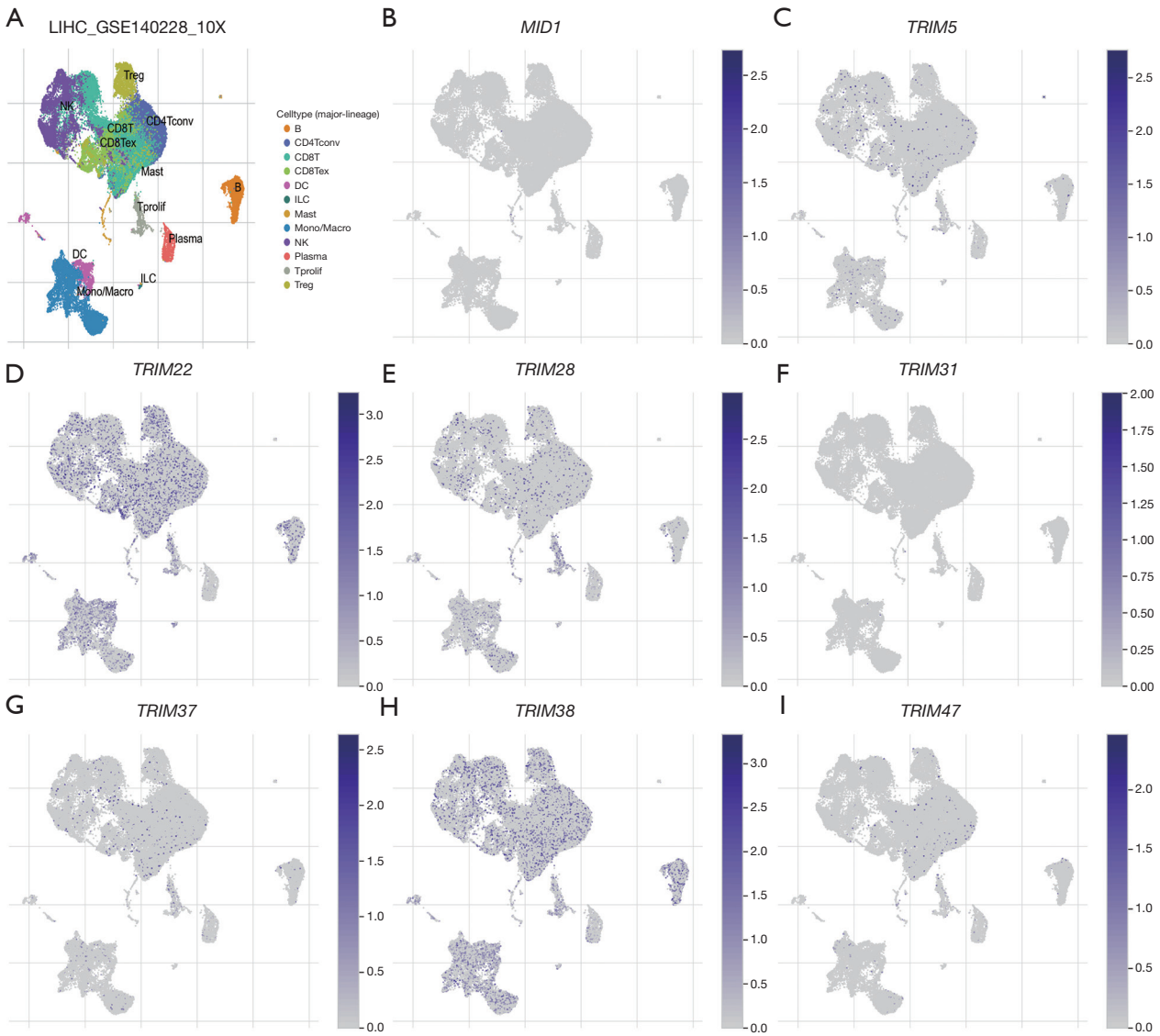

Figure 8 The cell types and their distribution in the LIHC_GSE140228 datasets. (A) The distribution of 8 *TRIM* genes in different cell types was analyzed using single-cell resolution in the LIHC_GSE140228 datasets. *MID1* (B), *TRIM5* (C), *TRIM22* (D), *TRIM28* (E), *TRIM31* (F), *TRIM37* (G), *TRIM38* (H), and *TRIM47* (I). LIHC, liver hepatocellular carcinoma; *TRIM*, tripartite-motif.

genes. The patients in cluster 1 showed a lower TNM stage. Similarly, cluster 1 had a better survival rate compared with that of cluster 2.

Furthermore, we analyzed and summarized the prognostic predictive role of *TRIM* family genes in HCC, and finally derived 9 prognostic risk signatures from *TRIM* genes, which effectively stratified the OS of HCC patients in the ICGC and TCGA cohorts into high- and low-risk groups. The risk score was found to be an independent prognostic factor for HCC patients in both univariate and multivariate cox regression models. The high- and low-risk groups were also related to distinct clustering subtypes, TNM stage, immune score, estimate score, tumor purity, and stromal score. Among these risk signatures, MID1, known as *TRIM18*, functions as an oncogene in melanoma (21). *TRIM31*, *TRIM28*, *TRIM37*, and *TRIM47* are involved in oncogenic regulation in HCC, gastric cancer, prostate cancer, and renal cell carcinoma, respectively (22-25). Interestingly, *TRIM37* has emerged as a tumor-suppressive regulator in various tumors in TRIM37 knock-out mice.

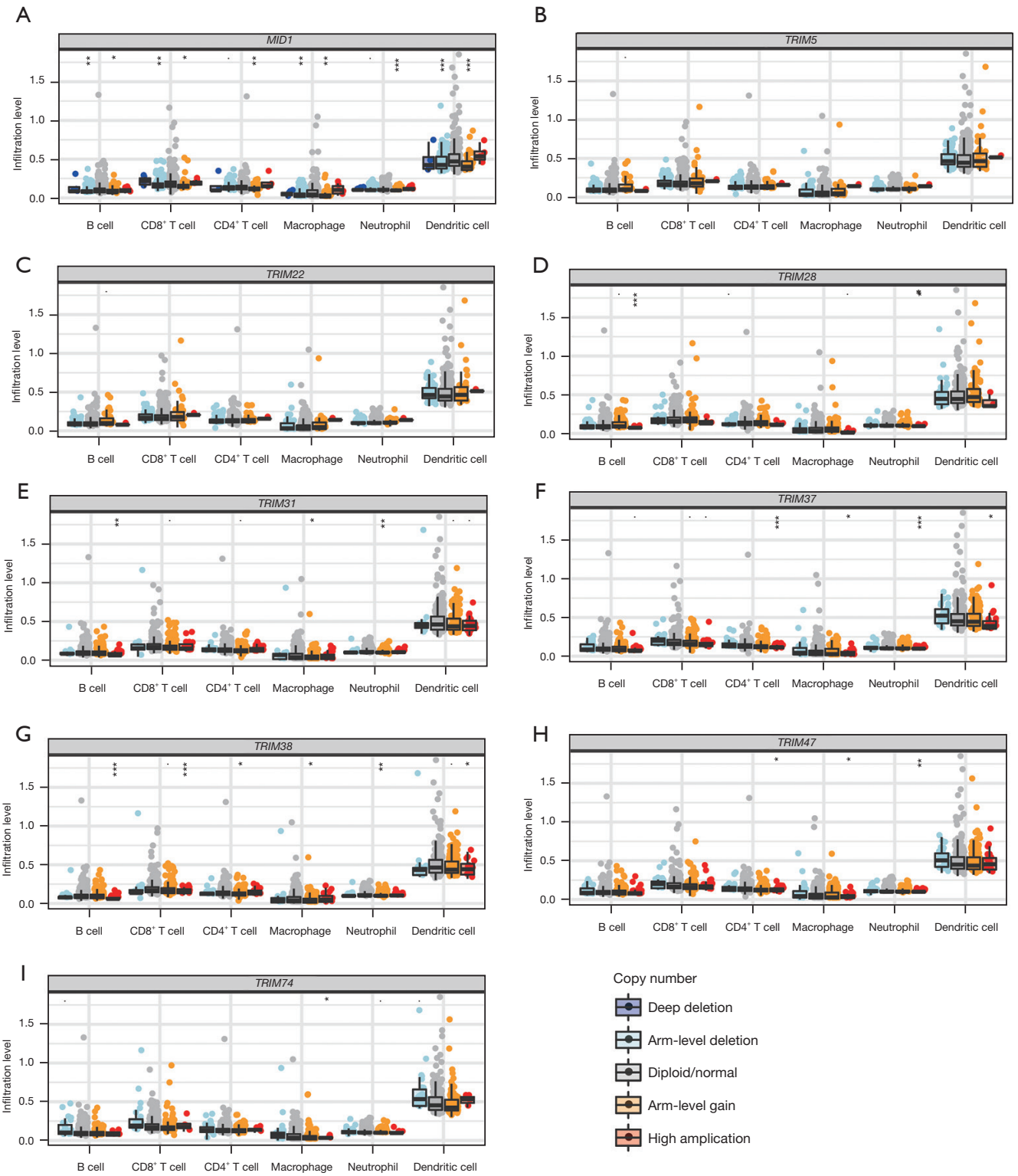

Figure 9 Effect of genetic alterations of *TRIM* gene-relevant signature on the immune cell infiltration. (A-I) *MID1* (A), *TRIM5* (B), *TRIM22* (C), *TRIM28* (D), *TRIM31* (E), *TRIM37* (F), *TRIM38* (G), *TRIM47* (H), and *TRIM74* (I). *P<0.05, **P<0.01, and ***P<0.001. *TRIM*, tripartite-motif.

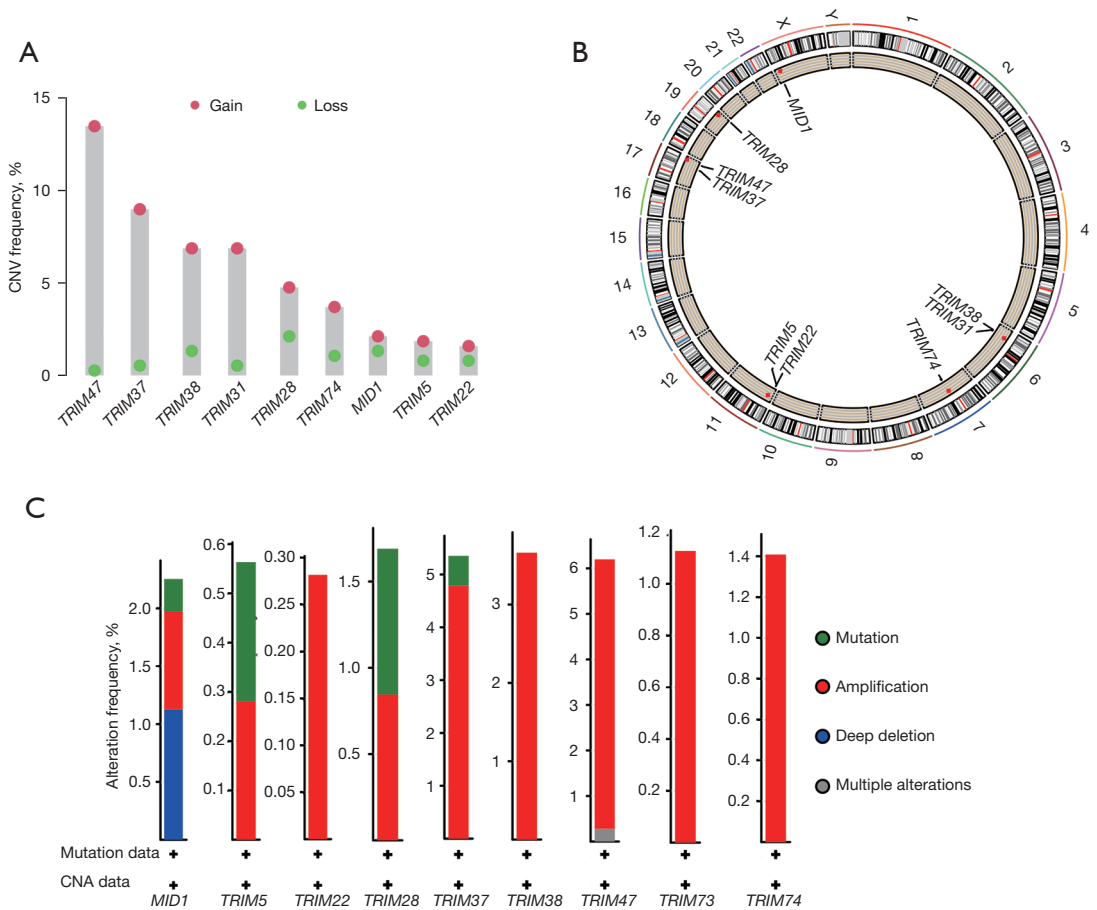

Figure 10 CNV frequency, location and alteration frequency of prognostic *TRIM* genes. CNV frequency of 9 prognostic *TRIM* genes (A). Location of *TRIM* genes on chromosomes (B). Alteration frequency of 9 prognostic *TRIM* genes (C). CNV, copy number variation; *TRIM*, tripartite-motif.

TRIM22 is a double-edged sword in that it is a tumor-suppressive regulator in endometrial cancer and gastric cancer (26,27) but is involved in oncogenic regulation in non-small cell lung cancer and chronic myeloid leukemia (28,29). There are few studies of *TRIM38* and *TRIM74* in tumors, and currently, research mainly focuses on innate immunity and inflammatory response (30,31). These findings demonstrated that deregulation of specific *TRIM* genes played separate functions in various cancers.

To further interrogate the mechanism of the role of *TRIM* family genes in HCC, we performed GSVA analysis and the results indicated that the malignant functional features of the tumor, including amino acid metabolism, fatty acid metabolism, and the drug metabolism cytochrome P450 pathway, were significantly enriched in cluster 1. This may be related to the high response of cluster 1 to sorafenib, TACE, as well as immunotherapy, which in turn had a better prognosis than cluster 2. Previous research has shown that *RIPK3*-dependent *TRIM28* inhibition in cancer cells leads to increased immunostimulatory cytokine production in the tumor microenvironment, which contributes to strong cytotoxic antitumor immunity (32). Liu *et al.* discovered that *TRIM28* knockdown increases sensitivity to etoposide by upregulating *E2F1* in non-small cell lung cancer (33). Previous study indicated that the expression level of *TRIM37* significantly increased in 354 HCC tissues and promoted peroxisomal matrix protein import via direct monoubiquitination of *PEX5* at *K464* and silencing of gene expression through monoubiquitination of histone *H2A* (34). Clinical data analysis has suggested that patients with high expression of *TRIM37* have more sorafenib resistance and shorter disease-free survival (DFS) and OS (P<0.01) (34). In addition, previous research reported that *TRIM47* overexpression played a

role in colorectal cancer chemoresistance in response to fluorouracil (5-FU) therapy (35). To date, *TRIM38* and *TRIM74* have been poorly studied in tumors, and their role in tumors may require more attention and investigation in the future. The above results were consistent with our study results; that is, patients in the high-risk group had a low response to both sorafenib treatment and TACE treatment, and had a poor prognosis. This suggested that for high-risk patients, new treatment strategies may need to be developed to improve survival rates. The predictive significance of the *TRIM* gene-relevant signatures was assessed in HCC patients and validated in the TCGA cohort, as well as the external GSE109211 and GSE104580 cohorts. The results showed that the *TRIM* gene-associated risk profiles could effectively predict the prognosis of HCC patients, allowing for more personalized treatment options and greater insight into the advancement of therapeutic techniques.

Previous studies have shown a close relationship between gene mutations and tumor development prognosis as well as treatment (36-38). Simultaneously, numerous research findings have revealed that the most common mutant gene mutations in HCC are, among others, *TP53* and *CTNNB1*, which are closely connected to the prognosis and therapies of HCC (36-38). At the same time, we also found that the most frequent type of non-nonsense mutation, whether in the low- or high-risk group, was a missense mutation. The top 3 genes with the highest frequency were *TP53*, *TTN*, and *CTNNB1*, respectively, which was consistent with previous studies (39,40). However, we found that the genes with the highest mutation frequency among high- and low-risk groups differed, with *CTNNB1* highest in the low-risk group and *TP53* highest in the high-risk group. Therefore, we may be able to distinguish whether a patient belongs to a high- or low-risk group by the specific gene mutated.

Although there are many models related to the prognosis and treatment of HCC, in this study, the risk prognostic model could distinguish well high and low risks by prognosis-related *TRIM* genes. In addition, the model could also distinguish well the response of HCC patients to immunotherapy, targeted therapy, and TACE, providing new insights and theories for precise, personalized treatment of HCC patients. In this study, the risk score based on the 9 *TRIM* gene-based risk signatures was shown to be strongly related to immune cell infiltration. These findings suggested that *TRIM* genes are involved in TIME regulation to some extent. In addition, the advent of ICIs has brought great benefits to cancer patients, and HCC patients are no exception, but not all patients can benefit from the treatment of ICIs. The immune checkpoint (*CTLA4*, *HAVCR2*, and *PDCD1*) expression levels of cluster 2 were significantly higher than that of cluster 1. The immunotherapy response of HCC is very low (about 10%), and our risk model could distinguish well which patients responded to immunotherapy, which in turn may improve the immunotherapy effect. To evaluate the response of HCC patients to immunotherapy, we employed the TIDE score, with the results showing that the low-risk score group had a low TIDE score but a high response to ICI treatment. Therefore, we proved that the *TRIM* family gene-based prognostic model could evaluate well the degree of benefit of immunotherapy in patients at different risk levels, leading to the implementation of personalized treatment strategies for different patients, ultimately benefiting patients.

Our research did, however, have some limitations. For instance, our findings were confirmed in the ICGC, TCGA, and GEO cohorts, but we didn't have any independent clinical sample data to support our claims and conclusions. Thus, the results of our research will need to be verified further, and we will continue to investigate *TRIM* gene correction and TIME in HCC in the future. In addition, the *TRIM* family's regulatory mechanism in TIME should be explored further in order to restructure TIME and improve HCC precision immunotherapy.

Conclusions

In conclusion, this research examined the prognostic significance, immune checkpoint correlations, TIME relevance, and potential regulatory mechanisms of *TRIM* genes in HCC. The risk score established from 9 *TRIM* gene-based signatures was found to be an independent prognostic indicator for HCC patients. TACE and ICI treatment were more likely to benefit patients with a low-risk score. The levels of immune cell infiltration in patients with HCC were strongly associated with the *TRIM* gene-based signatures. Further, many signaling pathways may be implicated in the regulation of the HCC immune microenvironment by the *TRIM* family. The identification of *TRIM* genes that contribute to biochemical pathways controlling tumor immune responses, as well as examining their regulatory processes and responses, could provide potential targets for enhancing HCC's immunotherapy responsiveness.

Acknowledgments

Funding: This work was funded by the National Natural Science Foundation of China (Nos. 81871909, 81702861), the "13th five-year Plan" Science and Education Strong Health Project Innovation team of Yangzhou (Nos. LJRC20181; YZCXTD201801), Provincial-level discipline leader of the NJPH (No. DTRC201809), and Beijing GanDanXiangZhao Public Welfare Foundation Project (No. GDXZ-08-19).

Footnote

Reporting Checklist: The authors have completed the TRIPOD reporting checklist. Available at https://jgo.amegroups.com/article/view/10.21037/jgo-22-619/rc

Conflicts of Interest: All authors have completed the ICMJE uniform disclosure form (available at https://jgo.amegroups.com/article/view/10.21037/jgo-22-619/coif). The authors have no conflicts of interest to declare.

Ethical Statement: The authors are accountable for all aspects of the work in ensuring that questions related to the accuracy or integrity of any part of the work are appropriately investigated and resolved. The study was conducted in accordance with the Declaration of Helsinki (as revised in 2013).

References

1. Yang JD, Hainaut P, Gores GJ, et al. A global view of hepatocellular carcinoma: trends, risk, prevention and management. Nat Rev Gastroenterol Hepatol 2019;16:589-604.
2. Ma KW, Cheung TT. Surgical resection of localized hepatocellular carcinoma: patient selection and special consideration. J Hepatocell Carcinoma 2017;4:1-9.
3. Xu DW, Wan P, Xia Q. Liver transplantation for hepatocellular carcinoma beyond the Milan criteria: A review. World J Gastroenterol 2016;22:3325-34.
4. Finn RS, Qin S, Ikeda M, et al. Atezolizumab plus Bevacizumab in Unresectable Hepatocellular Carcinoma. N Engl J Med 2020;382:1894-905.
5. Sanmamed MF, Chen L. A Paradigm Shift in Cancer Immunotherapy: From Enhancement to Normalization. Cell 2018;175:313-26.
6. Sprinzl MF, Galle PR. Current progress in immunotherapy of hepatocellular carcinoma. J Hepatol 2017;66:482-4.
7. Postow MA, Callahan MK, Wolchok JD. Immune Checkpoint Blockade in Cancer Therapy. J Clin Oncol 2015;33:1974-82.
8. Sharma P, Allison JP. Immune checkpoint targeting in cancer therapy: toward combination strategies with curative potential. Cell 2015;161:205-14.
9. Harding JJ. Immune checkpoint blockade in advanced hepatocellular carcinoma: an update and critical review of ongoing clinical trials. Future Oncol 2018;14:2293-302.
10. Short KM, Cox TC. Subclassification of the RBCC/TRIM superfamily reveals a novel motif necessary for microtubule binding. J Biol Chem 2006;281:8970-80.
11. Hatakeyama S. TRIM Family Proteins: Roles in Autophagy, Immunity, and Carcinogenesis. Trends Biochem Sci 2017;42:297-311.
12. Carthagena L, Bergamaschi A, Luna JM, et al. Human TRIM gene expression in response to interferons. PLoS One 2009;4:e4894.
13. Lv D, Li Y, Zhang W, et al. TRIM24 is an oncogenic transcriptional co-activator of STAT3 in glioblastoma. Nat Commun 2017;8:1454.
14. Czerwińska P, Mazurek S, Wiznerowicz M. The complexity of TRIM28 contribution to cancer. J Biomed Sci 2017;24:63.
15. Bhatnagar S, Gazin C, Chamberlain L, et al. TRIM37 is a new histone H2A ubiquitin ligase and breast cancer oncoprotein. Nature 2014;516:116-20.
16. Huang XQ, Zhang XF, Xia JH, et al. Tripartite motif-containing 3 (TRIM3) inhibits tumor growth and metastasis of liver cancer. Chin J Cancer 2017;36:77.
17. Li L, Dong L, Qu X, et al. Tripartite motif 16 inhibits hepatocellular carcinoma cell migration and invasion. Int J Oncol 2016;48:1639-49.
18. Yoshihara K, Shahmoradgoli M, Martínez E, et al. Inferring tumour purity and stromal and immune cell admixture from expression data. Nat Commun 2013;4:2612.
19. Jiang P, Gu S, Pan D, et al. Signatures of T cell

dysfunction and exclusion predict cancer immunotherapy response. Nat Med 2018;24:1550-8.
20. Balmain A. The critical roles of somatic mutations and environmental tumor-promoting agents in cancer risk. Nat Genet 2020;52:1139-43.
21. Xia Y, Zhao J, Yang C. Identification of key genes and pathways for melanoma in the TRIM family. Cancer Med 2020;9:8989-9005.
22. Guo P, Ma X, Zhao W, et al. TRIM31 is upregulated in hepatocellular carcinoma and promotes disease progression by inducing ubiquitination of TSC1-TSC2 complex. Oncogene 2018;37:478-88.
23. Fong KW, Zhao JC, Song B, et al. TRIM28 protects TRIM24 from SPOP-mediated degradation and promotes prostate cancer progression. Nat Commun 2018;9:5007.
24. Zhu H, Chen Y, Zhang J, et al. Knockdown of TRIM37 Promotes Apoptosis and Suppresses Tumor Growth in Gastric Cancer by Inactivation of the ERK1/2 Pathway. Onco Targets Ther 2020;13:5479-91.
25. Chen JX, Xu D, Cao JW, et al. TRIM47 promotes malignant progression of renal cell carcinoma by degrading P53 through ubiquitination. Cancer Cell Int 2021;21:129.
26. Naveed M, Ali A, Sheikh N, et al. Expression of TRIM22 mRNA in chronic hepatitis C patients treated with direct-acting antiviral drugs. APMIS 2020;128:326-34.
27. Zhou Z, Gao W, Yuan B, et al. TRIM22 inhibits the proliferation of gastric cancer cells through the Smad2 protein. Cell Death Discov 2021;7:234.
28. Liu L, Zhou XM, Yang FF, et al. TRIM22 confers poor prognosis and promotes epithelial-mesenchymal transition through regulation of AKT/GSK3β/β-catenin signaling in non-small cell lung cancer. Oncotarget 2017;8:62069-80.
29. Li L, Qi Y, Ma X, et al. TRIM22 knockdown suppresses chronic myeloid leukemia via inhibiting PI3K/Akt/mTOR signaling pathway. Cell Biol Int 2018;42:1192-9.
30. Hu MM, Shu HB. Multifaceted roles of TRIM38 in innate immune and inflammatory responses. Cell Mol Immunol 2017;14:331-8.
31. Hu MM, Xie XQ, Yang Q, et al. TRIM38 Negatively Regulates TLR3/4-Mediated Innate Immune and Inflammatory Responses by Two Sequential and Distinct Mechanisms. J Immunol 2015;195:4415-25.
32. Park HH, Kim HR, Park SY, et al. RIPK3 activation induces TRIM28 derepression in cancer cells and enhances the anti-tumor microenvironment. Mol Cancer 2021;20:107.
33. Liu L, Xiao L, Liang X, et al. TRIM28 knockdown increases sensitivity to etoposide by upregulating E2F1 in non-small cell lung cancer. Oncol Rep 2017;37:3597-605.
34. Tan G, Xie B, Yu N, et al. TRIM37 overexpression is associated with chemoresistance in hepatocellular carcinoma via activating the AKT signaling pathway. Int J Clin Oncol 2021;26:532-42.
35. Liang Q, Tang C, Tang M, et al. TRIM47 is up-regulated in colorectal cancer, promoting ubiquitination and degradation of SMAD4. J Exp Clin Cancer Res 2019;38:159.
36. Yang C, Huang X, Li Y, et al. Prognosis and personalized treatment prediction in TP53-mutant hepatocellular carcinoma: an in silico strategy towards precision oncology. Brief Bioinform 2021;22:bbaa164.
37. Huo J, Wu L, Zang Y. Construction and Validation of a Reliable Six-Gene Prognostic Signature Based on the TP53 Alteration for Hepatocellular Carcinoma. Front Oncol 2021;11:618976.
38. Liu Z, Zhang Y, Shi C, et al. A novel immune classification reveals distinct immune escape mechanism and genomic alterations: implications for immunotherapy in hepatocellular carcinoma. J Transl Med 2021;19:5.
39. Khemlina G, Ikeda S, Kurzrock R. The biology of Hepatocellular carcinoma: implications for genomic and immune therapies. Mol Cancer 2017;16:149.
40. Yin L, Zhou L, Xu R. Identification of Tumor Mutation Burden and Immune Infiltrates in Hepatocellular Carcinoma Based on Multi-Omics Analysis. Front Mol Biosci 2020;7:599142.

(English Language Editor: A. Muijlwijk)

Cite this article as: Cao J, Su B, Peng R, Tang H, Tu D, Tang Y, Zhou J, Jiang G, Jin S, Wang Q, Wang A, Liu R, Deng Q, Zhang C, Bai D. Bioinformatics analysis of immune infiltrates and tripartite motif (*TRIM*) family genes in hepatocellular carcinoma. J Gastrointest Oncol 2022;13(4):1942-1958. doi: 10.21037/jgo-22-619

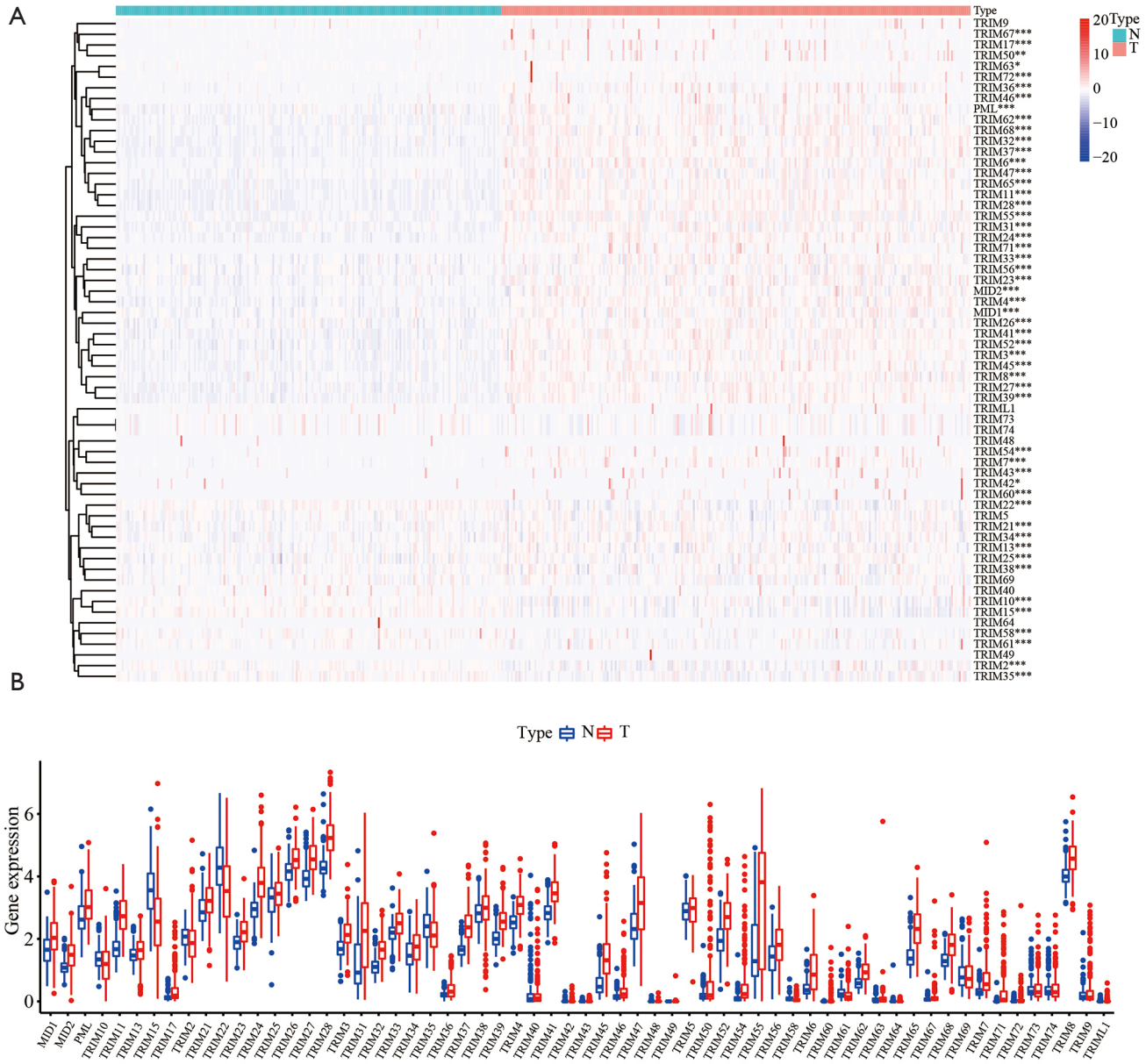

Figure S1 Upregulation of TRIM genes in HCC in ICGC cohort. Heatmap (A) and expression levels (B) of 62 TRIM genes. *P<0.05, **P<0.01, and ***P<0.001. TRIM, tripartite-motif; HCC, hepatocellular carcinoma; ICGC, International Cancer Genome Consortium.

https://dx.doi.org/10.21037/jgo-22-619

Table S1 The expression of all *TRIM* genes in HCC

Gene	conMean	treatMean	logFC	pValue
MID1	2.3272	3.6603	0.6533	<0.0001
MID2	1.1669	2.0190	0.7910	<0.0001
PML	6.1567	8.8012	0.5155	<0.0001
TRIM10	1.6589	1.5359	−0.1112	0.0006
TRIM11	2.5510	6.4281	1.3333	<0.0001
TRIM13	1.8944	2.2073	0.2206	0.0001
TRIM15	13.4980	7.4353	−0.8603	<0.0001
TRIM17	0.1045	0.3931	1.9112	<0.0001
TRIM2	3.2447	3.2776	0.0146	0.0002
TRIM21	7.2214	8.9731	0.3133	<0.0001
TRIM22	21.7251	14.5495	−0.5784	<0.0001
TRIM23	2.7480	3.9504	0.5236	<0.0001
TRIM24	6.9237	15.8774	1.1974	<0.0001
TRIM25	9.4121	10.6317	0.1758	0.0008
TRIM26	17.6007	23.8897	0.4408	<0.0001
TRIM27	15.6307	25.1302	0.6850	<0.0001
TRIM28	20.1263	42.7724	1.0876	<0.0001
TRIM3	2.4164	3.7850	0.6474	<0.0001
TRIM31	1.9820	7.3746	1.8956	<0.0001
TRIM32	1.2058	2.2773	0.9174	<0.0001
TRIM33	3.5734	4.9978	0.4840	<0.0001
TRIM34	2.0262	2.6108	0.3657	<0.0001
TRIM35	4.7165	4.1282	−0.1922	<0.0001
TRIM36	0.1685	0.3419	1.0209	<0.0001
TRIM37	2.1983	4.8216	1.1331	<0.0001
TRIM38	6.4133	7.8524	0.2921	0.0009
TRIM39	3.2459	5.4129	0.7378	<0.0001
TRIM4	4.8269	7.8473	0.7011	<0.0001
TRIM40	0.4712	0.3437	−0.4550	0.5527
TRIM41	6.4748	10.8891	0.7500	<0.0001
TRIM42	0.0040	0.0090	1.1693	0.0193
TRIM43	0.0011	0.0067	2.5721	0.0004
TRIM45	0.5743	2.3532	2.0346	<0.0001
TRIM46	0.1212	0.3280	1.4361	<0.0001
TRIM47	4.8948	10.5915	1.1136	<0.0001
TRIM48	0.0013	0.0013	−0.0647	0.5072
TRIM49	0.0000	0.0035	Inf	0.0694
TRIM5	6.6641	7.1118	0.0938	0.1080
TRIM50	0.1675	3.0263	4.1756	0.0015
TRIM52	3.1569	6.2149	0.9772	<0.0001
TRIM54	0.0845	0.8949	3.4051	<0.0001
TRIM55	3.5903	17.7277	2.3038	<0.0001
TRIM56	1.8245	2.8449	0.6408	<0.0001
TRIM58	0.0689	0.0423	−0.7061	<0.0001
TRIM6	0.3605	1.2824	1.8309	<0.0001
TRIM60	0.0001	0.0508	8.5018	<0.0001
TRIM61	0.2178	0.1920	−0.1818	<0.0001
TRIM62	0.5455	0.9907	0.8609	<0.0001
TRIM63	0.0404	0.2764	2.7751	0.0124
TRIM64	0.0078	0.0017	−2.2199	0.9238
TRIM65	1.8777	4.5920	1.2902	<0.0001
TRIM67	0.0554	0.1652	1.5758	<0.0001
TRIM68	1.5532	2.7472	0.8227	<0.0001
TRIM69	0.9438	0.9485	0.0072	0.3320
TRIM7	0.2728	0.9631	1.8201	<0.0001
TRIM71	0.0074	0.3440	5.5479	<0.0001
TRIM72	0.0116	0.0673	2.5391	<0.0001
TRIM73	0.3637	0.3947	0.1179	0.2986
TRIM74	0.3637	0.3947	0.1179	0.2986
TRIM8	16.0656	24.6381	0.6169	<0.0001
TRIM9	0.1845	0.4125	1.1608	0.2852
TRIML1	0.0073	0.0134	0.8848	0.9188

https://dx.doi.org/10.21037/jgo-22-619

Table S2 GSVA analysis to elucidate the potential regulatory mechanisms between the two subgroups

ID	logFC	AveExpr	P.Value	adj.P.Val
KEGG_LINOLEIC_ACID_METABOLISM	−0.4362	0.0560	<0.0001	<0.0001
KEGG_COMPLEMENT_AND_COAGULATION_CASCADES	−0.5351	0.0241	<0.0001	<0.0001
KEGG_HOMOLOGOUS_RECOMBINATION	0.4144	−0.0528	<0.0001	<0.0001
KEGG_PRIMARY_BILE_ACID_BIOSYNTHESIS	−0.6119	0.0168	<0.0001	<0.0001
KEGG_TRYPTOPHAN_METABOLISM	−0.4842	0.0175	<0.0001	<0.0001
KEGG_ABC_TRANSPORTERS	−0.3023	−0.0123	<0.0001	<0.0001
KEGG_BETA_ALANINE_METABOLISM	−0.4846	0.0198	<0.0001	<0.0001
KEGG_SPLICEOSOME	0.3668	−0.0469	<0.0001	<0.0001
KEGG_HISTIDINE_METABOLISM	−0.4064	0.0035	<0.0001	<0.0001
KEGG_DRUG_METABOLISM_CYTOCHROME_P450	−0.4921	0.0287	<0.0001	<0.0001
KEGG_ARACHIDONIC_ACID_METABOLISM	−0.2866	0.0366	<0.0001	<0.0001
KEGG_PHENYLALANINE_METABOLISM	−0.4250	0.0146	<0.0001	<0.0001
KEGG_PPAR_SIGNALING_PATHWAY	−0.3723	0.0278	<0.0001	<0.0001
KEGG_FATTY_ACID_METABOLISM	−0.5202	0.0120	<0.0001	<0.0001
KEGG_RETINOL_METABOLISM	−0.4790	0.0386	<0.0001	<0.0001
KEGG_PROPANOATE_METABOLISM	−0.4654	0.0061	<0.0001	<0.0001
KEGG_TYROSINE_METABOLISM	−0.3756	0.0143	<0.0001	<0.0001
KEGG_DNA_REPLICATION	0.4536	−0.0480	<0.0001	<0.0001
KEGG_GLYCINE_SERINE_AND_THREONINE_METABOLISM	−0.4740	0.0085	<0.0001	<0.0001
KEGG_VALINE_LEUCINE_AND_ISOLEUCINE_DEGRADATION	−0.4999	0.0107	<0.0001	<0.0001
KEGG_METABOLISM_OF_XENOBIOTICS_BY_CYTOCHROME_P450	−0.4452	0.0278	<0.0001	<0.0001
KEGG_BUTANOATE_METABOLISM	−0.4414	0.0236	<0.0001	<0.0001
KEGG_STEROID_HORMONE_BIOSYNTHESIS	−0.4255	0.0340	<0.0001	<0.0001
KEGG_STARCH_AND_SUCROSE_METABOLISM	−0.3732	0.0159	<0.0001	<0.0001
KEGG_PYRUVATE_METABOLISM	−0.3380	0.0052	<0.0001	<0.0001
KEGG_ALANINE_ASPARTATE_AND_GLUTAMATE_METABOLISM	−0.3489	0.0130	<0.0001	<0.0001
KEGG_PEROXISOME	−0.3760	0.0035	<0.0001	<0.0001
KEGG_ARGININE_AND_PROLINE_METABOLISM	−0.3389	0.0119	<0.0001	<0.0001
KEGG_CELL_CYCLE	0.2833	−0.0425	<0.0001	<0.0001
KEGG_BASE_EXCISION_REPAIR	0.2861	−0.0547	<0.0001	<0.0001
KEGG_RNA_DEGRADATION	0.2455	−0.0447	<0.0001	<0.0001
KEGG_OLFACTORY_TRANSDUCTION	−0.1981	0.1215	<0.0001	<0.0001
KEGG_ASCORBATE_AND_ALDARATE_METABOLISM	−0.4993	0.0309	<0.0001	<0.0001
KEGG_NITROGEN_METABOLISM	−0.2892	0.0337	<0.0001	<0.0001
KEGG_DRUG_METABOLISM_OTHER_ENZYMES	−0.3605	0.0143	<0.0001	<0.0001
KEGG_ADIPOCYTOKINE_SIGNALING_PATHWAY	−0.1837	−0.0184	<0.0001	<0.0001
KEGG_PENTOSE_AND_GLUCURONATE_INTERCONVERSIONS	−0.4425	0.0253	<0.0001	<0.0001
KEGG_ALPHA_LINOLENIC_ACID_METABOLISM	−0.2423	0.0566	<0.0001	<0.0001
KEGG_NEUROACTIVE_LIGAND_RECEPTOR_INTERACTION	−0.1584	0.0431	<0.0001	<0.0001
KEGG_FOLATE_BIOSYNTHESIS	−0.3437	0.0017	<0.0001	<0.0001
KEGG_PROXIMAL_TUBULE_BICARBONATE_RECLAMATION	−0.2409	0.0302	<0.0001	<0.0001
KEGG_MISMATCH_REPAIR	0.3222	−0.0470	<0.0001	<0.0001
KEGG_CYSTEINE_AND_METHIONINE_METABOLISM	−0.2067	−0.0193	<0.0001	<0.0001
KEGG_UBIQUITIN_MEDIATED_PROTEOLYSIS	0.1727	−0.0432	<0.0001	<0.0001
KEGG_NUCLEOTIDE_EXCISION_REPAIR	0.2386	−0.0505	<0.0001	<0.0001
KEGG_RENIN_ANGIOTENSIN_SYSTEM	−0.2404	0.0294	<0.0001	<0.0001
KEGG_RNA_POLYMERASE	0.2721	−0.0561	<0.0001	<0.0001
KEGG_PYRIMIDINE_METABOLISM	0.1930	−0.0445	<0.0001	<0.0001
KEGG_GLYCOLYSIS_GLUCONEOGENESIS	−0.2388	0.0118	<0.0001	<0.0001
KEGG_GLYCOSAMINOGLYCAN_BIOSYNTHESIS_KERATAN_SULFATE	0.2046	−0.0113	<0.0001	<0.0001
KEGG_PURINE_METABOLISM	0.1181	−0.0305	<0.0001	<0.0001
KEGG_PORPHYRIN_AND_CHLOROPHYLL_METABOLISM	−0.3215	−0.0056	<0.0001	<0.0001
KEGG_LYSINE_DEGRADATION	−0.2463	−0.0319	<0.0001	<0.0001
KEGG_OOCYTE_MEIOSIS	0.1546	−0.0246	<0.0001	<0.0001
KEGG_BIOSYNTHESIS_OF_UNSATURATED_FATTY_ACIDS	−0.2928	−0.0033	<0.0001	<0.0001
KEGG_GLYCEROLIPID_METABOLISM	−0.1413	0.0045	<0.0001	<0.0001
KEGG_BLADDER_CANCER	0.1553	−0.0287	<0.0001	<0.0001
KEGG_VASOPRESSIN_REGULATED_WATER_REABSORPTION	0.1656	−0.0266	<0.0001	<0.0001
KEGG_TAURINE_AND_HYPOTAURINE_METABOLISM	−0.1956	0.0123	<0.0001	<0.0001
KEGG_PATHOGENIC_ESCHERICHIA_COLI_INFECTION	0.1904	−0.0226	<0.0001	<0.0001
KEGG_NICOTINATE_AND_NICOTINAMIDE_METABOLISM	−0.1734	−0.0065	<0.0001	<0.0001
KEGG_GLYOXYLATE_AND_DICARBOXYLATE_METABOLISM	−0.2582	−0.0179	<0.0001	<0.0001
KEGG_ENDOCYTOSIS	0.1132	−0.0290	<0.0001	<0.0001
KEGG_NOTCH_SIGNALING_PATHWAY	0.1637	−0.0331	<0.0001	<0.0001
KEGG_CHRONIC_MYELOID_LEUKEMIA	0.1469	−0.0356	<0.0001	<0.0001
KEGG_MATURITY_ONSET_DIABETES_OF_THE_YOUNG	−0.2106	0.0634	<0.0001	<0.0001
KEGG_PROGESTERONE_MEDIATED_OOCYTE_MATURATION	0.1317	−0.0235	<0.0001	<0.0001
KEGG_VIBRIO_CHOLERAE_INFECTION	0.1555	−0.0246	<0.0001	<0.0001
KEGG_RIBOSOME	0.3317	−0.0444	<0.0001	<0.0001
KEGG_MTOR_SIGNALING_PATHWAY	0.1126	−0.0330	<0.0001	<0.0001
KEGG_CITRATE_CYCLE_TCA_CYCLE	−0.2601	−0.0140	<0.0001	<0.0001
KEGG_FC_GAMMA_R_MEDIATED_PHAGOCYTOSIS	0.1620	−0.0202	<0.0001	<0.0001
KEGG_PRION_DISEASES	−0.1604	−0.0142	<0.0001	<0.0001
KEGG_ALDOSTERONE_REGULATED_SODIUM_REABSORPTION	−0.1090	0.0144	<0.0001	<0.0001
KEGG_CALCIUM_SIGNALING_PATHWAY	−0.1111	0.0175	<0.0001	<0.0001
KEGG_PANCREATIC_CANCER	0.1387	−0.0314	<0.0001	<0.0001
KEGG_NON_HOMOLOGOUS_END_JOINING	0.1840	−0.0353	<0.0001	<0.0001
KEGG_THYROID_CANCER	0.1095	−0.0426	<0.0001	<0.0001
KEGG_NON_SMALL_CELL_LUNG_CANCER	0.1096	−0.0325	<0.0001	0.0001
KEGG_GLYCOSAMINOGLYCAN_BIOSYNTHESIS_HEPARAN_SULFATE	0.1164	0.0023	<0.0002	0.0001
KEGG_NEUROTROPHIN_SIGNALING_PATHWAY	0.1118	−0.0292	0.0001	0.0002
KEGG_ERBB_SIGNALING_PATHWAY	0.1003	−0.0169	0.0001	0.0002
KEGG_BASAL_TRANSCRIPTION_FACTORS	0.1289	−0.0379	0.0001	0.0002
KEGG_GLYCOSYLPHOSPHATIDYLINOSITOL_GPI_ANCHOR_BIOSYNTHESIS	0.1491	−0.0471	0.0001	0.0002
KEGG_GLYCOSAMINOGLYCAN_BIOSYNTHESIS_CHONDROITIN_SULFATE	0.1576	−0.0157	0.0001	0.0003
KEGG_RENAL_CELL_CARCINOMA	0.1315	−0.0216	0.0002	0.0003
KEGG_PANTOTHENATE_AND_COA_BIOSYNTHESIS	−0.1478	−0.0195	0.0002	0.0005
KEGG_SYSTEMIC_LUPUS_ERYTHEMATOSUS	−0.1909	−0.0013	0.0003	0.0006
KEGG_GLUTATHIONE_METABOLISM	−0.1349	−0.0093	0.0004	0.0009
KEGG_ONE_CARBON_POOL_BY_FOLATE	−0.1441	−0.0258	0.0005	0.0009
KEGG_GALACTOSE_METABOLISM	−0.1080	0.0034	0.0006	0.0011
KEGG_SNARE_INTERACTIONS_IN_VESICULAR_TRANSPORT	0.1004	−0.0327	0.0014	0.0027
KEGG_AUTOIMMUNE_THYROID_DISEASE	−0.1667	0.0217	0.0019	0.0035
KEGG_SULFUR_METABOLISM	−0.1121	−0.0188	0.0035	0.0062
KEGG_CYTOKINE_CYTOKINE_RECEPTOR_INTERACTION	−0.1077	0.0127	0.0058	0.0100
KEGG_CELL_ADHESION_MOLECULES_CAMS	−0.1107	0.0035	0.0060	0.0103
KEGG_RIBOFLAVIN_METABOLISM	0.1104	−0.0333	0.0062	0.0104
KEGG_AMINOACYL_TRNA_BIOSYNTHESIS	0.1325	−0.0469	0.0092	0.0146
KEGG_CIRCADIAN_RHYTHM_MAMMAL	−0.1121	−0.0384	0.0098	0.0153
KEGG_ASTHMA	−0.1477	0.0069	0.0103	0.0159
KEGG_GRAFT_VERSUS_HOST_DISEASE	−0.1461	−0.0085	0.0210	0.0309
KEGG_ALLOGRAFT_REJECTION	−0.1442	−0.0097	0.0256	0.0373

https://dx.doi.org/10.21037/jgo-22-619

Table S3 Prognostic nine TRIM genes

Gene	Coef
MID1	0.2866
TRIM22	–0.2776
TRIM28	0.0285
TRIM31	0.1564
TRIM37	0.5382
TRIM38	–0.1205
TRIM47	0.1407
TRIM5	–0.1805
TRIM74	–0.9219

Table S4 Risk score for all TCGA data

ID	Exclusion	Dysfunction	riskScore	Risk
TCGA-2Y-A9H3	–0.0474	0.1729	–49.3037	Low
TCGA-2Y-A9GU	–0.0283	–0.0595	–45.6506	Low
TCGA-FV-A3R3	0.0016	0.0780	–25.7199	Low
TCGA-2Y-A9GT	–0.1133	0.1553	–14.4872	Low
TCGA-RC-A7SF	0.0027	–0.0308	–12.2966	Low
TCGA-5R-AA1C	0.0081	–0.1849	–11.2011	Low
TCGA-2Y-A9GZ	–0.0310	0.0087	–8.9811	Low
TCGA-ZS-A9CF	–0.0443	–0.0676	–8.6015	Low
TCGA-ED-A5KG	–0.1825	0.2566	–7.1056	Low
TCGA-LG-A9QD	–0.0386	0.0088	–6.9790	Low
TCGA-G3-AAV3	–0.0393	0.0945	–5.0507	Low
TCGA-DD-A4NV	–0.0107	0.0569	–4.3457	Low
TCGA-ZS-A9CE	–0.0040	0.0088	–4.1545	Low
TCGA-K7-A5RF	–0.0908	0.2246	–4.0518	Low
TCGA-DD-A73G	0.0315	0.0656	–1.9289	Low
TCGA-WX-AA46	–0.0293	–0.0343	–1.6475	Low
TCGA-DD-AAE2	–0.0683	0.0630	–1.1195	Low
TCGA-DD-A4NI	–0.0923	–0.0071	–0.7051	Low
TCGA-UB-A7MF	–0.0987	0.1404	–0.1059	Low
TCGA-DD-AAE7	–0.0341	0.0628	–0.0399	Low
TCGA-EP-A12J	–0.0387	0.0018	–0.0217	Low
TCGA-DD-AAE4	–0.0108	0.0394	0.7199	High
TCGA-DD-AADK	0.0292	0.0299	0.7691	High
TCGA-G3-A7M8	–0.0309	0.0196	0.8261	High
TCGA-ES-A2HS	0.0376	0.0594	1.3293	High
TCGA-UB-AA0V	–0.0022	0.0173	1.5663	High
TCGA-DD-AADS	–0.0098	0.1034	1.7363	High
TCGA-DD-A113	–0.0018	–0.0684	2.2476	High
TCGA-UB-A7ME	–0.0416	0.0942	2.4707	High
TCGA-2Y-A9GW	–0.1168	0.0859	2.5219	High
TCGA-2Y-A9H1	0.0125	0.0484	2.7754	High
TCGA-DD-A73F	–0.1009	0.1551	2.9532	High
TCGA-2Y-A9H6	–0.0518	0.1375	3.0770	High
TCGA-DD-A4NL	–0.0425	0.0619	3.1210	High
TCGA-K7-A6G5	–0.0156	0.0430	3.1394	High
TCGA-LG-A6GG	–0.0199	–0.0384	3.2767	High
TCGA-G3-AAV0	0.0066	0.0990	3.4712	High
TCGA-ED-A82E	0.0374	–0.0066	3.8014	High
TCGA-DD-AAVX	–0.0609	0.0809	4.0699	High
TCGA-G3-A3CH	–0.0394	0.0582	4.1358	High
TCGA-G3-A5SK	–0.0617	–0.0617	4.1507	High
TCGA-BC-A10X	0.0040	–0.0119	4.3283	High
TCGA-MR-A520	–0.0346	–0.0784	4.3670	High
TCGA-EP-A26S	–0.0033	–0.0683	4.5219	High
TCGA-DD-A11C	0.0044	–0.0303	5.6144	High
TCGA-G3-A3CI	–0.0516	0.0535	5.8799	High
TCGA-DD-A73A	–0.0788	0.0224	5.9362	High
TCGA-DD-A11B	–0.0209	–0.1642	6.0507	High
TCGA-FV-A495	0.0461	0.1868	6.1468	High
TCGA-WQ-AB4B	0.0142	–0.0100	6.3425	High
TCGA-DD-A4ND	–0.0066	0.0436	6.4321	High
TCGA-ZS-A9CG	0.0049	–0.0553	6.5373	High
TCGA-ES-A2HT	0.0041	0.0666	6.5914	High
TCGA-2Y-A9GV	–0.0919	0.0599	6.7530	High
TCGA-DD-AAEG	0.0187	–0.0519	6.8438	High
TCGA-KR-A7K2	–0.0116	0.0542	7.0492	High
TCGA-DD-AAVR	–0.0418	0.0522	7.2502	High
TCGA-DD-A4NK	–0.0430	0.0197	7.5605	High
TCGA-PD-A5DF	0.0162	–0.0401	7.6052	High
TCGA-2Y-A9HB	–0.0880	0.0848	7.7086	High
TCGA-DD-A3A1	–0.0059	0.0065	8.1417	High
TCGA-FV-A3I0	0.0304	0.0477	8.1706	High
TCGA-DD-AAE3	0.0284	0.0006	8.4894	High
TCGA-G3-A6UC	–0.0475	–0.0144	8.7629	High
TCGA-5C-A9VG	0.0467	–0.1069	8.7828	High
TCGA-G3-A3CG	–0.0462	0.0066	9.0318	High
TCGA-2Y-A9H9	–0.0498	0.0371	9.1955	High
TCGA-EP-A3JL	–0.0205	0.0575	9.3135	High
TCGA-DD-AACK	–0.0127	–0.1191	9.3311	High
TCGA-ED-A4XI	–0.0559	0.1675	9.5345	High
TCGA-DD-AAED	–0.0236	–0.0681	9.6136	High
TCGA-DD-AACC	–0.1869	0.2904	9.6498	High
TCGA-5R-AAAM	–0.0141	0.1120	9.7452	High
TCGA-DD-A39V	0.0321	0.0105	9.7919	High
TCGA-DD-A11D	–0.0371	0.0481	9.9768	High
TCGA-DD-A4NE	0.0165	–0.1350	10.0410	High
TCGA-5C-A9VH	0.0083	–0.0040	10.1745	High
TCGA-DD-AACD	0.0164	0.0093	10.4713	High
TCGA-K7-A5RG	–0.1837	0.2402	10.6122	High
TCGA-DD-AAD2	0.0210	0.1095	10.7700	High
TCGA-DD-AAEK	–0.0931	0.1204	10.8463	High
TCGA-DD-A3A9	0.0527	0.0954	10.8841	High
TCGA-O8-A75V	–0.0335	0.0687	10.9630	High
TCGA-DD-AAVQ	–0.1064	0.2493	11.0546	High
TCGA-G3-AAUZ	0.0048	0.1033	11.1211	High
TCGA-DD-AAEH	–0.0626	0.0880	11.4667	High
TCGA-DD-A73B	0.0017	–0.1862	11.4723	High
TCGA-2Y-A9H5	–0.0277	0.0224	11.8374	High
TCGA-G3-A25T	0.0423	0.0380	12.2692	High
TCGA-DD-AACZ	–0.0758	–0.0618	12.3836	High
TCGA-GJ-A9DB	–0.0164	0.0513	12.4499	High
TCGA-G3-A3CK	–0.0302	–0.0706	12.5069	High
TCGA-DD-A1ED	–0.0614	0.0573	12.6590	High
TCGA-KR-A7K0	–0.0113	–0.0244	12.7702	High
TCGA-DD-AAD3	0.0098	0.0458	12.8558	High
TCGA-3K-AAZ8	–0.0510	0.0442	12.8906	High
TCGA-EP-A2KC	–0.0236	–0.0809	13.1717	High
TCGA-G3-AAV2	0.0261	0.0296	13.2008	High
TCGA-G3-AAV5	0.0352	–0.0780	13.2622	High
TCGA-2Y-A9H2	–0.0158	0.0491	13.2923	High
TCGA-XR-A8TD	–0.0864	0.0944	13.5165	High
TCGA-RC-A7S9	0.0146	–0.0440	13.5989	High
TCGA-ED-A627	–0.0212	0.2243	13.6795	High
TCGA-DD-AAD8	–0.0228	–0.0528	13.6966	High
TCGA-DD-AADA	–0.0408	–0.0407	13.6971	High
TCGA-XR-A8TG	–0.0113	–0.0581	13.9032	High
TCGA-DD-AACO	0.0194	–0.0051	13.9748	High
TCGA-DD-A4NS	0.0179	0.1750	14.0901	High
TCGA-2Y-A9GX	–0.0399	0.1317	14.1431	High
TCGA-YA-A8S7	–0.0327	0.0863	14.6573	High
TCGA-DD-AADF	0.0171	–0.0235	14.7114	High
TCGA-CC-5260	0.0270	0.0650	14.9802	High
TCGA-BC-A69I	0.0211	0.0915	14.9951	High
TCGA-G3-A25V	–0.0369	0.1178	15.1010	High
TCGA-DD-A4NP	0.0198	0.0001	15.1884	High
TCGA-FV-A2QR	0.0009	–0.0206	15.3318	High
TCGA-DD-A1EE	–0.0298	–0.0888	15.3649	High
TCGA-DD-A3A5	0.0143	0.0626	15.3840	High
TCGA-DD-AAW1	–0.0282	–0.0241	15.5194	High
TCGA-DD-A4NN	0.0525	–0.0546	15.6017	High
TCGA-DD-AAVW	–0.0175	–0.0118	15.7967	High
TCGA-BC-A5W4	0.0425	0.0174	16.1183	High
TCGA-DD-AACN	0.0163	–0.0488	16.1690	High
TCGA-UB-AA0U	0.0107	–0.0400	16.1917	High
TCGA-DD-AACY	–0.0233	0.0078	16.3513	High
TCGA-DD-AACW	0.0336	–0.0660	16.3846	High
TCGA-KR-A7K8	–0.0538	0.1509	16.4430	High
TCGA-GJ-A3OU	–0.2045	0.2154	16.5132	High
TCGA-DD-A1EB	–0.0438	0.0155	16.5358	High
TCGA-DD-AADY	0.0026	–0.0949	16.5388	High
TCGA-LG-A9QC	–0.0105	–0.0263	16.7782	High
TCGA-DD-AAD1	–0.0171	0.1293	16.8467	High
TCGA-FV-A3R2	–0.0092	–0.0088	16.8733	High
TCGA-DD-AAVY	–0.0192	–0.0819	17.0350	High
TCGA-DD-AAW0	–0.0650	0.0225	17.2182	High
TCGA-DD-A4NF	–0.0016	–0.0878	17.4766	High
TCGA-DD-A4NJ	–0.0408	–0.0589	17.6363	High
TCGA-CC-A8HS	0.0254	–0.1110	17.6735	High
TCGA-HP-A5MZ	–0.0402	0.0823	17.7588	High
TCGA-DD-A11A	–0.0296	–0.1176	17.8499	High
TCGA-DD-A3A8	0.0292	–0.0196	17.8818	High
TCGA-DD-A4NA	–0.0195	0.0035	18.0012	High
TCGA-DD-AACQ	–0.0112	0.0560	18.1104	High
TCGA-MI-A75C	0.0056	0.0004	18.1866	High
TCGA-G3-A7M7	0.0087	–0.0180	18.2393	High
TCGA-ZS-A9CD	–0.0124	0.0705	18.3647	High
TCGA-DD-AAEI	–0.0240	0.0392	18.3789	High
TCGA-DD-AADV	0.0171	–0.0497	18.4240	High
TCGA-DD-A73C	–0.0261	–0.0161	18.5181	High
TCGA-BC-4073	–0.0804	–0.0009	18.5490	High
TCGA-DD-A3A6	0.0724	0.1434	18.5962	High
TCGA-DD-A1EG	–0.0380	0.0294	18.6194	High
TCGA-MI-A75E	–0.0103	0.1863	18.7210	High
TCGA-4R-AA8I	–0.0474	–0.0195	19.0536	High
TCGA-RC-A7SH	–0.0142	0.0613	19.0774	High
TCGA-DD-A4NR	–0.1546	0.2374	19.1824	High
TCGA-CC-A9FS	–0.0061	–0.0708	19.2683	High
TCGA-DD-AADM	0.0485	–0.0364	19.2798	High
TCGA-UB-A7MD	–0.0492	0.0982	19.3661	High
TCGA-DD-AADG	0.0164	–0.0124	19.4552	High
TCGA-DD-AADP	–0.0050	–0.0781	19.5100	High
TCGA-DD-A1EC	–0.1259	0.1826	19.5392	High
TCGA-DD-A73E	0.0212	–0.0072	19.7399	High
TCGA-FV-A496	–0.0267	–0.0554	19.8703	High
TCGA-CC-5261	–0.0072	0.0137	19.8791	High
TCGA-CC-A3M9	0.0365	0.1520	19.9448	High
TCGA-RC-A6M4	0.0256	–0.0504	19.9468	High
TCGA-DD-AAE1	–0.0093	–0.0723	20.0012	High
TCGA-DD-AAD0	0.0107	–0.0028	20.0163	High
TCGA-2Y-A9H4	0.0037	0.0098	20.0555	High
TCGA-G3-AAV4	0.0085	–0.0376	20.1092	High
TCGA-5C-AAPD	–0.0332	0.1339	20.1679	High
TCGA-DD-A115	0.0042	0.1068	20.2658	High
TCGA-G3-A25Y	0.0284	–0.0204	20.2727	High
TCGA-DD-AAEA	–0.0119	0.0390	20.3918	High
TCGA-K7-AAU7	0.0321	0.0047	20.4091	High
TCGA-BW-A5NO	–0.0080	–0.0106	20.6713	High
TCGA-DD-A1EK	–0.0513	0.0568	20.7388	High
TCGA-ED-A7XP	–0.0294	–0.1107	20.7799	High
TCGA-FV-A2QQ	–0.0130	–0.0072	20.8270	High
TCGA-DD-A4NO	–0.0081	–0.0432	21.1019	High
TCGA-DD-AADQ	–0.0059	–0.0688	21.1156	High
TCGA-DD-AADU	0.0047	–0.0233	21.1901	High
TCGA-DD-A1EI	0.0441	–0.0705	21.2066	High
TCGA-ED-A7XO	0.0071	0.1014	21.2980	High
TCGA-EP-A3RK	–0.0419	0.0989	21.5279	High
TCGA-ED-A7PX	0.0458	0.0165	21.5419	High
TCGA-DD-A39W	–0.0084	–0.0197	21.6660	High
TCGA-G3-A5SM	–0.0396	0.0954	21.8344	High
TCGA-BC-A8YO	–0.0609	–0.0283	21.9492	High
TCGA-WX-AA44	0.0176	–0.0447	22.5134	High
TCGA-ED-A97K	0.0002	0.0556	22.5578	High
TCGA-DD-A118	–0.0012	–0.0115	22.5898	High
TCGA-CC-5262	0.0543	0.0823	22.6086	High
TCGA-DD-A116	0.0284	0.0755	22.6417	High
TCGA-DD-AAE9	0.0195	–0.0532	22.8720	High
TCGA-BD-A3ER	–0.0281	0.0665	22.9885	High
TCGA-CC-5258	0.0434	–0.1473	23.0318	High
TCGA-DD-A3A2	–0.0154	–0.0245	23.5287	High
TCGA-G3-A5SL	0.0122	–0.1855	23.6051	High
TCGA-G3-A3CJ	0.0216	–0.0260	23.6632	High
TCGA-DD-AAC9	–0.0095	0.1043	23.7211	High
TCGA-DD-A1EF	–0.0063	–0.0685	23.9588	High
TCGA-BC-A216	–0.0206	–0.0046	24.0985	High
TCGA-DD-A119	0.0377	–0.1074	24.1091	High
TCGA-DD-A4NH	–0.0330	–0.0539	24.3243	High
TCGA-DD-AACS	–0.0002	–0.0405	24.3873	High
TCGA-DD-AAVZ	–0.0338	–0.1349	24.4536	High
TCGA-FV-A3I1	–0.0415	0.0878	24.5146	High
TCGA-CC-A7IH	–0.0031	–0.1068	24.6912	High
TCGA-FV-A4ZQ	–0.0523	0.0314	24.7356	High
TCGA-EP-A2KA	–0.0149	0.0540	24.8030	High
TCGA-DD-A1EA	–0.0657	0.0093	24.8794	High
TCGA-XR-A8TE	0.0153	–0.0229	24.9121	High
TCGA-NI-A4U2	–0.0089	–0.0854	25.0381	High
TCGA-2Y-A9H7	0.0318	–0.0449	25.1356	High
TCGA-DD-AACF	–0.0094	–0.0188	25.1689	High
TCGA-DD-A3A4	–0.0016	–0.0878	25.2018	High
TCGA-G3-A25Z	0.0028	–0.0538	25.2398	High
TCGA-DD-AAVU	0.0711	–0.0268	25.3713	High
TCGA-DD-AAW3	0.0000	–0.0832	25.4125	High
TCGA-DD-AA3A	0.0701	–0.0543	25.6446	High
TCGA-RC-A6M5	0.0447	0.1154	25.6784	High
TCGA-G3-A5SJ	–0.0116	–0.0542	25.7010	High
TCGA-MI-A75G	0.0036	–0.0371	25.7071	High
TCGA-DD-A4NG	–0.0095	–0.1048	25.7547	High
TCGA-CC-A7IJ	0.1029	0.0829	25.8625	High
TCGA-DD-AACH	0.0268	–0.0199	25.8967	High
TCGA-RC-A7SK	0.0106	–0.0008	25.9722	High
TCGA-DD-AACT	–0.0413	0.0759	26.3330	High
TCGA-DD-AACB	–0.0123	0.0447	26.3387	High
TCGA-XR-A8TF	0.0076	–0.1052	26.4413	High
TCGA-DD-A4NB	0.1096	0.0401	26.4728	High
TCGA-G3-A25S	0.0188	–0.0268	26.6004	High
TCGA-CC-A3MA	0.0736	–0.0305	26.7830	High
TCGA-XR-A8TC	–0.0329	–0.1350	27.3507	High
TCGA-DD-AADI	0.0135	0.0601	27.3773	High
TCGA-DD-A3A3	0.0295	–0.0035	27.6860	High
TCGA-ED-A66Y	0.0220	–0.0243	27.7812	High
TCGA-DD-A39X	0.0404	0.0099	27.8564	High
TCGA-DD-AADJ	0.0326	0.0090	27.9148	High
TCGA-FV-A23B	–0.0254	–0.0337	28.0196	High
TCGA-BD-A3EP	–0.0656	0.2221	28.1053	High
TCGA-DD-AADB	–0.0280	–0.0318	28.3524	High
TCGA-G3-A7M9	0.0498	–0.0387	28.4961	High
TCGA-2Y-A9GY	–0.0199	0.0363	28.5320	High
TCGA-DD-AAW2	0.0101	–0.0923	28.5450	High
TCGA-BC-A217	0.0067	–0.0381	28.5789	High
TCGA-ED-A66X	0.0024	0.0409	28.6213	High
TCGA-5R-AA1D	0.0704	0.0215	28.7820	High
TCGA-G3-A25U	–0.0165	–0.1015	28.8305	High
TCGA-DD-AACL	0.0004	0.0413	29.0358	High
TCGA-ED-A459	–0.0022	–0.0147	29.0371	High
TCGA-CC-A3MB	0.0220	–0.1102	29.0499	High
TCGA-CC-A7IL	0.0024	–0.0545	29.1815	High
TCGA-G3-A5SI	0.0381	–0.2036	29.2852	High
TCGA-G3-A7M5	–0.0115	0.0616	29.4252	High
TCGA-G3-A7M6	0.0284	0.0042	29.4369	High
TCGA-QA-A7B7	0.0004	–0.0986	29.5061	High
TCGA-2Y-A9HA	–0.0102	–0.0697	29.5287	High
TCGA-DD-AAVS	–0.0215	–0.0525	29.6345	High
TCGA-NI-A8LF	–0.0086	–0.0039	29.6568	High
TCGA-CC-A1HT	–0.0227	0.0241	29.7124	High
TCGA-DD-AADR	0.0435	–0.1800	29.9311	High
TCGA-DD-AAC8	0.0311	–0.0678	29.9700	High
TCGA-CC-A7IF	–0.0006	0.0067	30.1526	High
TCGA-GJ-A6C0	–0.0336	0.0448	30.2994	High
TCGA-DD-AAVV	–0.0456	0.0879	30.3323	High
TCGA-DD-AACE	–0.0347	–0.0346	30.3382	High
TCGA-DD-AAVP	0.0409	0.0207	30.3759	High
TCGA-CC-A8HV	0.0216	–0.0607	30.3793	High
TCGA-DD-AACU	–0.0219	0.0743	30.6044	High
TCGA-DD-AADL	0.0180	–0.0718	30.7073	High
TCGA-BC-A3KF	–0.0098	–0.0396	31.0627	High
TCGA-CC-A7II	0.0926	–0.0400	31.2218	High
TCGA-DD-AACA	0.0600	–0.0399	31.4012	High
TCGA-MR-A8JO	0.0213	0.0923	31.4561	High
TCGA-BC-4072	–0.0437	0.0319	31.5583	High
TCGA-CC-A3MC	0.0173	–0.0280	32.3777	High
TCGA-UB-A7MB	0.0129	–0.0670	32.4113	High
TCGA-G3-AAV7	0.0230	–0.0992	32.6433	High
TCGA-DD-AAE0	0.0796	–0.0066	32.7135	High
TCGA-UB-A7MA	0.0362	–0.0105	32.8377	High
TCGA-DD-AAD5	0.0443	–0.0093	32.9321	High
TCGA-DD-AAEE	0.0397	–0.0567	33.2638	High
TCGA-DD-A39Z	0.0522	–0.0187	33.5105	High
TCGA-BC-A10Z	–0.0277	–0.0949	33.6723	High
TCGA-DD-AACG	0.0515	–0.0673	34.2712	High
TCGA-G3-AAV1	–0.0139	–0.1208	34.2880	High
TCGA-RC-A7SB	0.0145	–0.0259	34.3350	High
TCGA-CC-A5UE	0.0523	–0.0813	34.6014	High
TCGA-UB-A7MC	–0.0306	–0.1417	34.8137	High
TCGA-DD-AADW	0.0384	–0.1257	34.9712	High
TCGA-CC-5264	0.0106	–0.1209	35.0059	High
TCGA-DD-AACI	–0.0456	0.0903	35.1311	High
TCGA-KR-A7K7	0.0215	0.0352	35.4139	High
TCGA-EP-A2KB	0.0414	–0.0823	36.5702	High
TCGA-CC-A5UD	0.0727	–0.0328	36.6436	High
TCGA-CC-A5UC	0.0995	–0.1433	36.7329	High
TCGA-WJ-A86L	–0.0282	0.0257	36.8622	High
TCGA-BC-A69H	0.0753	0.0196	37.0553	High
TCGA-FV-A4ZP	0.0329	0.0718	37.2668	High
TCGA-DD-AACV	0.0194	–0.0929	37.3916	High
TCGA-RC-A6M6	0.0596	0.0099	37.6020	High
TCGA-BC-A3KG	0.0194	–0.1622	38.3392	High
TCGA-CC-A8HT	0.0207	–0.1002	38.4502	High
TCGA-DD-AADN	–0.0023	0.0650	38.7824	High
TCGA-CC-A7IK	0.0199	–0.1122	38.8375	High
TCGA-G3-AAV6	0.0930	–0.0825	39.1850	High
TCGA-DD-A4NQ	0.0000	–0.0768	39.4062	High
TCGA-CC-5263	0.0045	–0.0665	39.6828	High
TCGA-DD-A114	–0.0473	0.1071	40.4127	High
TCGA-RG-A7D4	–0.0317	–0.0430	40.4401	High
TCGA-DD-A1EH	0.0152	–0.1410	40.6905	High
TCGA-DD-A1EL	0.0407	–0.1758	40.7280	High
TCGA-CC-A9FW	0.0321	–0.0341	40.7736	High
TCGA-DD-A39Y	0.0733	–0.0996	40.8844	High
TCGA-DD-A1EJ	0.0436	–0.1342	41.2159	High
TCGA-DD-AACP	0.0821	0.0067	41.5167	High
TCGA-CC-A7IG	0.0508	0.0226	41.7250	High
TCGA-2Y-A9H0	0.0001	–0.0156	41.7732	High
TCGA-ED-A8O5	0.0259	–0.0985	42.1507	High
TCGA-DD-AACX	–0.0142	0.0080	42.3864	High
TCGA-CC-A8HU	0.0192	–0.0685	42.9054	High
TCGA-DD-A3A7	0.0189	0.0290	44.4750	High
TCGA-CC-A7IE	0.0288	–0.0998	45.6339	High
TCGA-G3-A25X	0.0773	0.0174	45.7224	High
TCGA-CC-A123	0.0573	–0.0540	46.0509	High
TCGA-DD-AADD	0.0234	–0.0626	47.2176	High
TCGA-ED-A8O6	0.0103	–0.0409	47.3197	High
TCGA-DD-AAE6	0.0207	0.0430	47.3457	High
TCGA-DD-AADC	0.0562	–0.1562	48.4493	High
TCGA-CC-5259	0.0203	–0.0304	48.8348	High
TCGA-DD-AACJ	0.0126	–0.0483	48.9603	High
TCGA-DD-A73D	–0.0021	–0.1584	49.1750	High
TCGA-DD-AADO	0.0129	–0.0009	49.4529	High
TCGA-ED-A7PY	–0.0025	–0.0846	52.3838	High
TCGA-DD-AAD6	0.0266	–0.1093	54.3818	High
TCGA-ED-A7PZ	0.0397	–0.0262	55.1359	High

https://dx.doi.org/10.21037/jgo-22-619

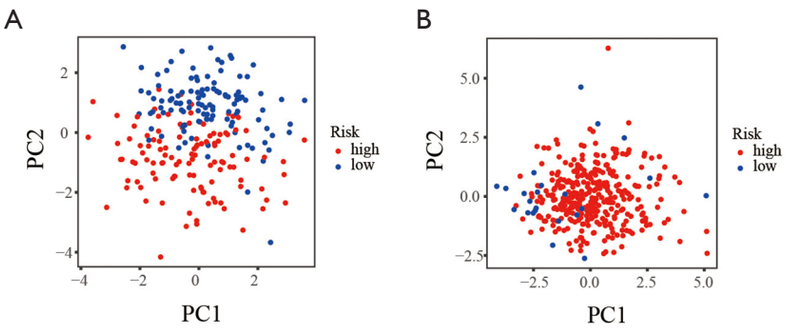

Figure S2 Principal component analysis of the total mRNA expression profile in patients with HCC. (A) ICGC dataset (231), (B) TCGA dataset (370). HCC, hepatocellular carcinoma; ICGC, International Cancer Genome Consortium; TCGA, The Cancer Genome Atlas.

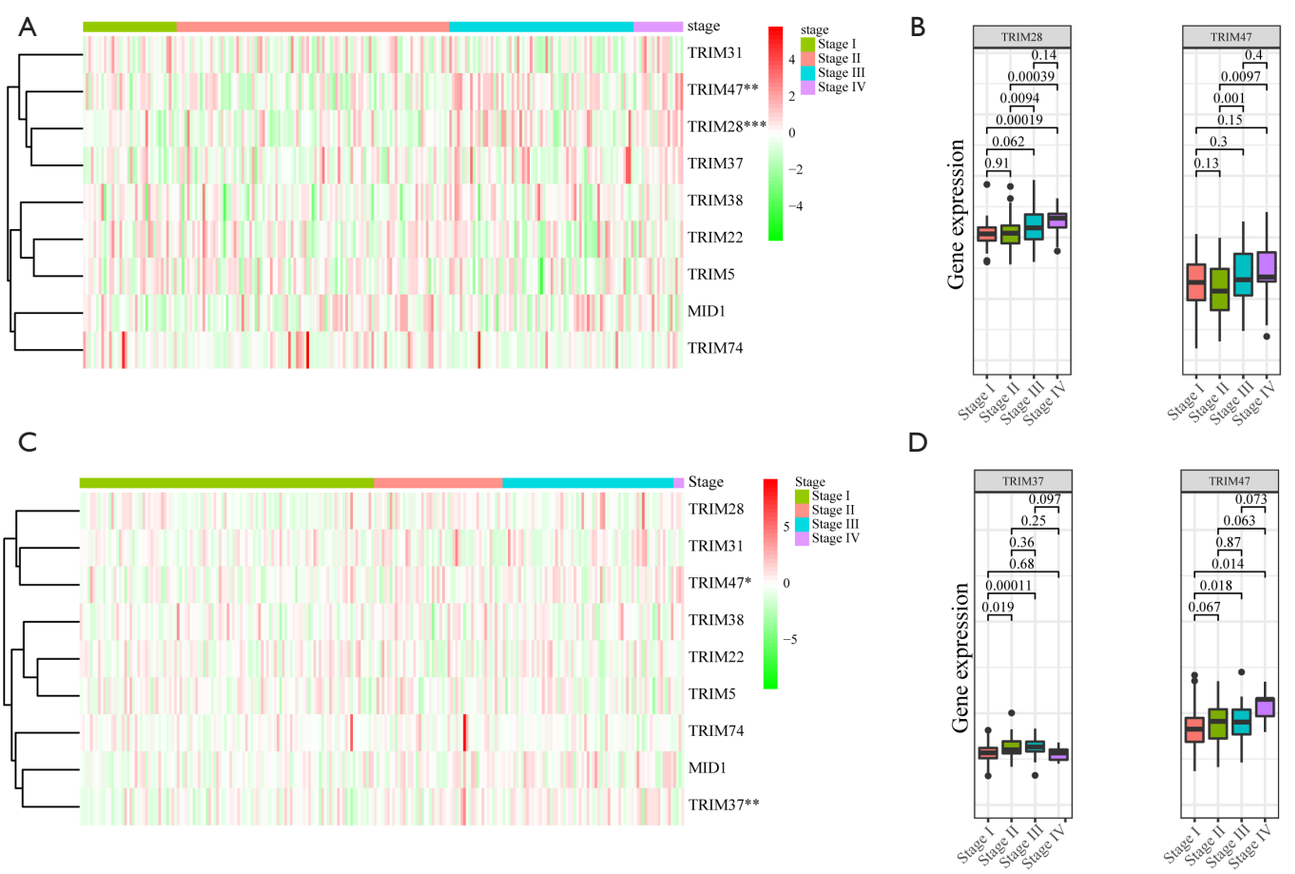

Figure S3 Expression of 9 prognostic TRIM genes in different TNM stages. (A,B) ICGC dataset; (C,D) TCGA dataset. *P<0.05, **P<0.01, and ***P<0.001. TRIM, tripartite-motif; ICGC, International Cancer Genome Consortium; TCGA, The Cancer Genome Atlas.

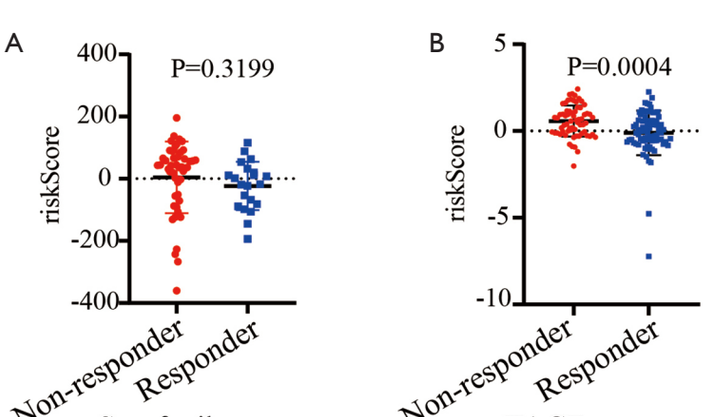

Figure S4 Prognostic risk scores correlated with sorafenib treatment and TACE treatment. (A) Sorafenib treatment; (B) TACE treatment. TACE, transarterial chemotherapy embolization.

https://dx.doi.org/10.21037/jgo-22-619

Table S5 Prognostic risk scores correlated with sorafenib treatment

ID	riskScore	Risk	Response
GSM2935384	−360.5127	Low	Non-responder
GSM2935326	−266.9720	Low	Non-responder
GSM2935402	−242.7517	Low	Non-responder
GSM2935416	−226.8208	Low	Non-responder
GSM2935378	−130.6702	Low	Non-responder
GSM2935395	−123.8420	Low	Non-responder
GSM2935362	−123.5592	Low	Non-responder
GSM2935304	−106.2238	Low	Non-responder
GSM2935355	−91.8073	Low	Non-responder
GSM2935397	−87.6133	Low	Non-responder
GSM2935380	−70.9621	Low	Non-responder
GSM2935292	−55.8145	Low	Non-responder
GSM2935350	−50.8004	Low	Non-responder
GSM2935340	−10.8910	Low	Non-responder
GSM2935389	−2.3515	Low	Non-responder
GSM2935414	2.0936	High	Non-responder
GSM2935297	20.2977	High	Non-responder
GSM2935351	23.0205	High	Non-responder
GSM2935323	24.3236	High	Non-responder
GSM2935328	30.6782	High	Non-responder
GSM2935307	36.0293	High	Non-responder
GSM2935353	36.1191	High	Non-responder
GSM2935407	37.9594	High	Non-responder
GSM2935338	42.4778	High	Non-responder
GSM2935370	43.1468	High	Non-responder
GSM2935342	44.0766	High	Non-responder
GSM2935360	44.5883	High	Non-responder
GSM2935356	55.4280	High	Non-responder
GSM2935296	56.8567	High	Non-responder
GSM2935401	58.0768	High	Non-responder
GSM2935403	59.7852	High	Non-responder
GSM2935320	63.6101	High	Non-responder
GSM2935303	65.7638	High	Non-responder
GSM2935386	66.0764	High	Non-responder
GSM2935331	70.3566	High	Non-responder
GSM2935289	85.0381	High	Non-responder
GSM2935330	88.0587	High	Non-responder
GSM2935314	90.7093	High	Non-responder
GSM2935317	92.2376	High	Non-responder
GSM2935365	104.9897	High	Non-responder
GSM2935327	110.6924	High	Non-responder
GSM2935305	120.1545	High	Non-responder
GSM2935301	121.9265	High	Non-responder
GSM2935302	126.8631	High	Non-responder
GSM2935311	136.7348	High	Non-responder
GSM2935329	195.8208	High	Non-responder
GSM2935313	−193.8786	Low	Responder
GSM2935279	−144.9182	Low	Responder
GSM2935394	−106.0342	Low	Responder
GSM2935288	−98.4313	Low	Responder
GSM2935280	−89.0318	Low	Responder
GSM2935406	−81.4792	Low	Responder
GSM2935385	−67.9112	Low	Responder
GSM2935411	−53.9916	Low	Responder
GSM2935281	−22.7166	Low	Responder
GSM2935333	−19.0166	Low	Responder
GSM2935310	−17.8325	Low	Responder
GSM2935413	1.9529	High	Responder
GSM2935415	7.8781	High	Responder
GSM2935282	10.8473	High	Responder
GSM2935361	11.4204	High	Responder
GSM2935285	19.6260	High	Responder
GSM2935396	32.1272	High	Responder
GSM2935392	53.3647	High	Responder
GSM2935409	62.7018	High	Responder
GSM2935300	88.6393	High	Responder
GSM2935405	115.5827	High	Responder

https://dx.doi.org/10.21037/jgo-22-619

Table S6 Prognostic risk scores correlated with Sorafenib treatment and TACE treatment

id	riskScore	risk	responder
GSM2803756	-2.0163	low	non-responder
GSM2803739	-1.1911	low	non-responder
GSM2803800	-0.9370	low	non-responder
GSM2803752	-0.8942	low	non-responder
GSM2803747	-0.7745	low	non-responder
GSM2803792	-0.3672	low	non-responder
GSM2803738	-0.3559	low	non-responder
GSM2803786	-0.3010	low	non-responder
GSM2803765	-0.2988	low	non-responder
GSM2803788	-0.2933	low	non-responder
GSM2803742	-0.2682	low	non-responder
GSM2803768	-0.2405	low	non-responder
GSM2803780	-0.2104	low	non-responder
GSM2803784	-0.1980	low	non-responder
GSM2803791	-0.1464	low	non-responder
GSM2803759	-0.1228	low	non-responder
GSM2803736	-0.1119	low	non-responder
GSM2803745	-0.0562	low	non-responder
GSM2803776	-0.0407	low	non-responder
GSM2803771	-0.0290	low	non-responder
GSM2803777	0.0099	low	non-responder
GSM2803764	0.0515	low	non-responder
GSM2803772	0.0981	low	non-responder
GSM2803744	0.1543	low	non-responder
GSM2803783	0.1767	low	non-responder
GSM2803775	0.1945	low	non-responder
GSM2803794	0.3324	low	non-responder
GSM2803767	0.3550	low	non-responder
GSM2803751	0.3713	low	non-responder
GSM2803797	0.3890	low	non-responder
GSM2803793	0.4574	low	non-responder
GSM2803770	0.4944	low	non-responder
GSM2803760	0.5732	high	non-responder
GSM2803748	0.6140	high	non-responder
GSM2803779	0.6665	high	non-responder
GSM2803750	0.6906	high	non-responder
GSM2803740	0.7522	high	non-responder
GSM2803749	0.7751	high	non-responder
GSM2803746	0.7779	high	non-responder
GSM2803782	0.8685	high	non-responder
GSM2803773	0.8790	high	non-responder
GSM2803741	0.9386	high	non-responder
GSM2803753	0.9496	high	non-responder
GSM2803766	0.9600	high	non-responder
GSM2803755	0.9653	high	non-responder
GSM2803801	0.9665	high	non-responder
GSM2803761	1.0067	high	non-responder
GSM2803799	1.0301	high	non-responder
GSM2803798	1.1131	high	non-responder
GSM2803737	1.1334	high	non-responder
GSM2803778	1.1620	high	non-responder
GSM2803754	1.3480	high	non-responder
GSM2803758	1.3742	high	non-responder
GSM2803795	1.5149	high	non-responder
GSM2803790	1.5834	high	non-responder
GSM2803762	1.6215	high	non-responder
GSM2803785	1.6765	high	non-responder
GSM2803757	1.7183	high	non-responder
GSM2803796	1.7663	high	non-responder
GSM2803774	1.7796	high	non-responder
GSM2803743	1.8133	high	non-responder
GSM2803763	1.8644	high	non-responder
GSM2803769	2.0558	high	non-responder
GSM2803781	2.1016	high	non-responder
GSM2803789	2.1436	high	non-responder
GSM2803787	2.4178	high	non-responder
GSM2803709	-7.2321	low	responder
GSM2803734	-4.7626	low	responder
GSM2803655	-1.8194	low	responder
GSM2803695	-1.7293	low	responder
GSM2803679	-1.4777	low	responder
GSM2803715	-1.3736	low	responder
GSM2803682	-1.1624	low	responder
GSM2803704	-1.0597	low	responder
GSM2803674	-1.0376	low	responder
GSM2803721	-0.9981	low	responder
GSM2803670	-0.9307	low	responder
GSM2803671	-0.8857	low	responder
GSM2803723	-0.8292	low	responder
GSM2803705	-0.7900	low	responder
GSM2803689	-0.7610	low	responder
GSM2803688	-0.7389	low	responder
GSM2803664	-0.6850	low	responder
GSM2803728	-0.6304	low	responder
GSM2803696	-0.6146	low	responder
GSM2803673	-0.5658	low	responder
GSM2803724	-0.5632	low	responder
GSM2803719	-0.5481	low	responder
GSM2803720	-0.5407	low	responder
GSM2803702	-0.5404	low	responder
GSM2803676	-0.5136	low	responder
GSM2803732	-0.5046	low	responder
GSM2803685	-0.4953	low	responder
GSM2803686	-0.4770	low	responder
GSM2803662	-0.4727	low	responder
GSM2803735	-0.4581	low	responder
GSM2803693	-0.4477	low	responder
GSM2803717	-0.4018	low	responder
GSM2803678	-0.3976	low	responder
GSM2803700	-0.3152	low	responder
GSM2803697	-0.2857	low	responder
GSM2803680	-0.2494	low	responder
GSM2803716	-0.2079	low	responder
GSM2803672	-0.1175	low	responder
GSM2803690	-0.1055	low	responder
GSM2803657	-0.0843	low	responder
GSM2803667	-0.0118	low	responder
GSM2803718	-0.0029	low	responder
GSM2803698	-0.0011	low	responder
GSM2803733	0.0595	low	responder
GSM2803687	0.0664	low	responder
GSM2803681	0.0781	low	responder
GSM2803684	0.1246	low	responder
GSM2803710	0.1591	low	responder
GSM2803669	0.1761	low	responder
GSM2803729	0.2021	low	responder
GSM2803722	0.2509	low	responder
GSM2803701	0.3419	low	responder
GSM2803677	0.3516	low	responder
GSM2803711	0.3664	low	responder
GSM2803694	0.3712	low	responder
GSM2803691	0.3879	low	responder
GSM2803675	0.4749	low	responder
GSM2803713	0.5477	low	responder
GSM2803666	0.5613	low	responder
GSM2803714	0.5724	high	responder
GSM2803663	0.5818	high	responder
GSM2803661	0.5962	high	responder
GSM2803656	0.6022	high	responder
GSM2803692	0.6147	high	responder
GSM2803727	0.8035	high	responder
GSM2803726	0.8210	high	responder
GSM2803668	0.9388	high	responder
GSM2803707	1.0595	high	responder
GSM2803660	1.0819	high	responder
GSM2803659	1.0863	high	responder
GSM2803708	1.1031	high	responder
GSM2803658	1.1051	high	responder
GSM2803683	1.1233	high	responder
GSM2803725	1.1621	high	responder
GSM2803712	1.2094	high	responder
GSM2803731	1.3620	high	responder
GSM2803706	1.5474	high	responder
GSM2803730	1.5793	high	responder
GSM2803665	1.6264	high	responder
GSM2803699	1.9248	high	responder
GSM2803703	2.2595	high	responder

https://dx.doi.org/10.21037/jgo-22-619

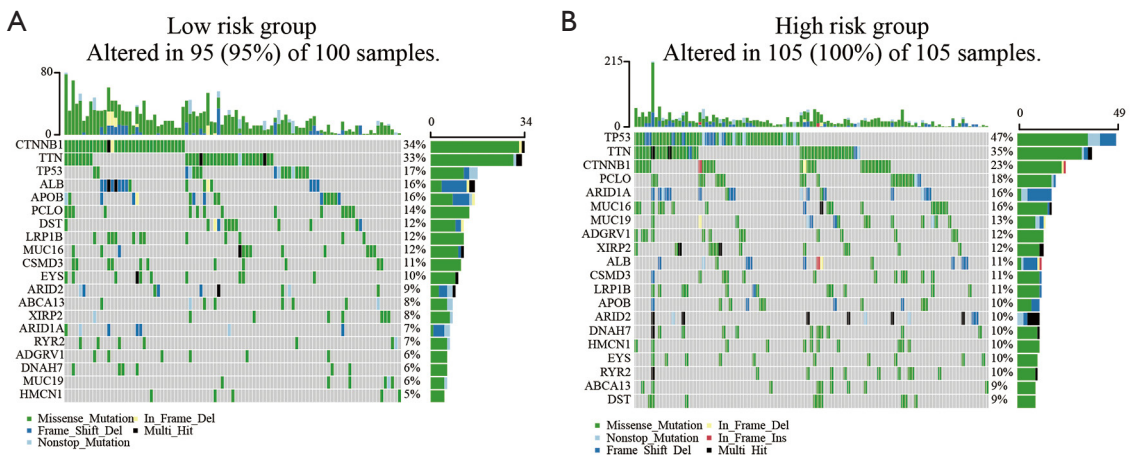

Figure S5 Landscape of mutation information of high- and low-risk HCC sample in waterfall plot. (A) Low-risk; (B) high-risk. HCC, hepatocellular carcinoma.

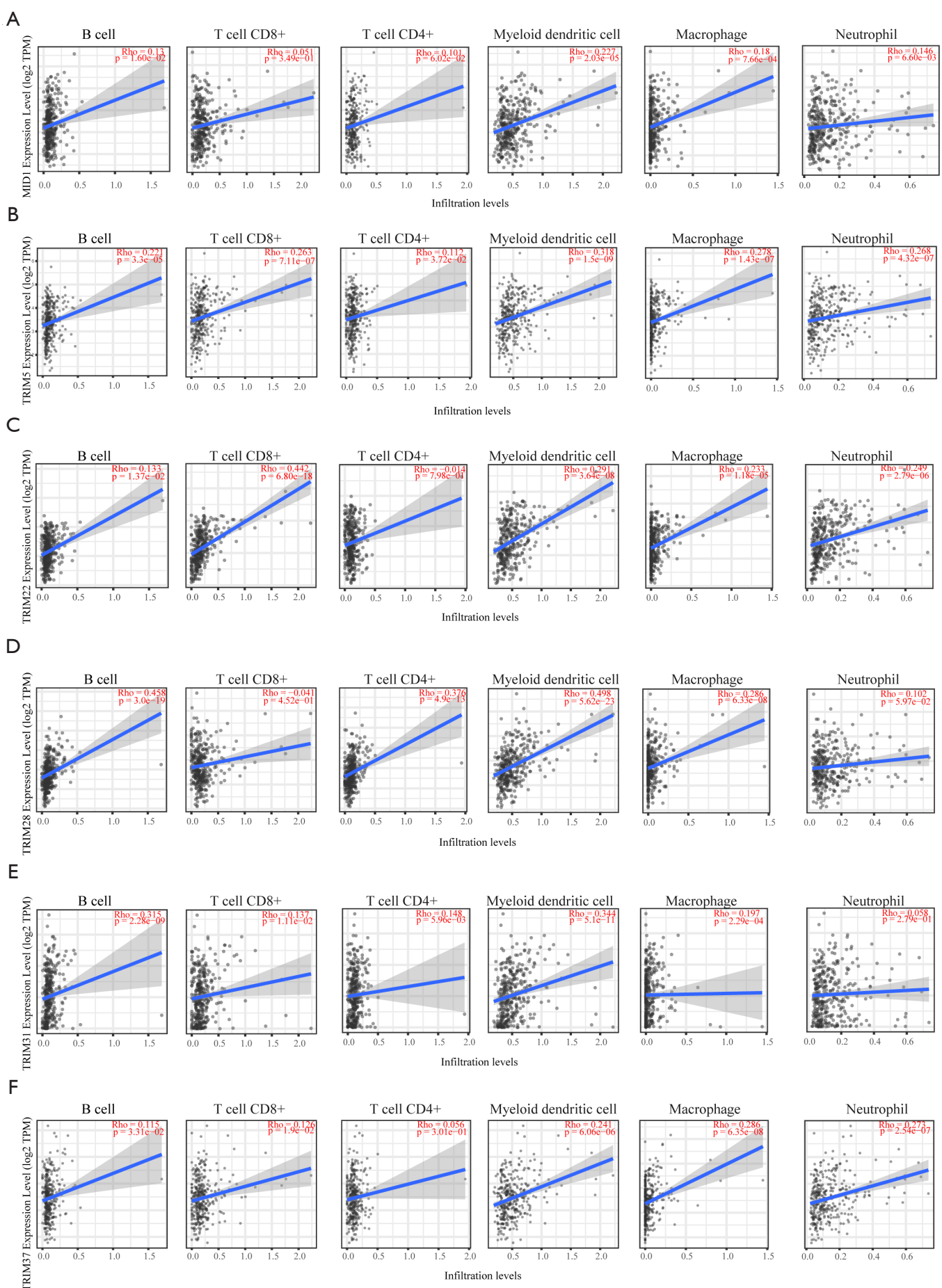

Figure S6 Relationship of the 9 TRIM genes with infiltration levels of 6 immune cell types. (A) MID1, (B) TRIM5, (C) TRIM22, (D) TRIM28, (E) TRIM31, (F) TRIM37. TRIM, tripartite-motif.

https://dx.doi.org/10.21037/jgo-22-619

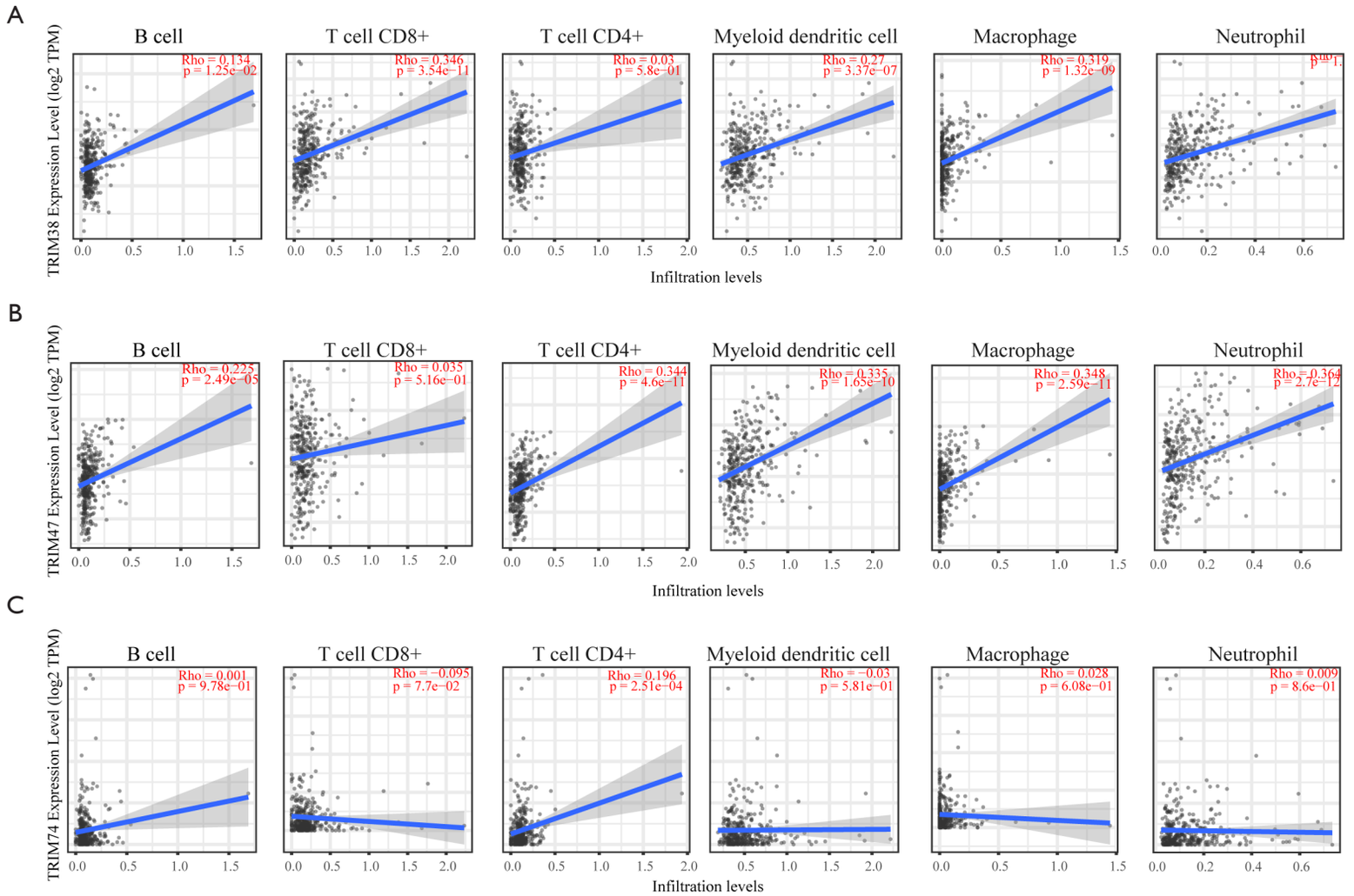

Figure S7 Relationship of the 9 TRIM genes with infiltration levels of 6 immune cell types. (A) TRIM38, (B) TRIM47, and (C) TRIM74. TRIM, tripartite-motif.

https://dx.doi.org/10.21037/jgo-22-619